Article:
Zhou, Y, Ge, S, Jin, L et al. (8 more authors) (2019) A novel CO_2-responsive systemic signaling pathway controlling plant mycorrhizal symbiosis. New Phytologist, 224 (1). pp. 106-116. ISSN 0028-646X

https://doi.org/10.1111/nph.15917

A novel CO_2-responsive systemic signaling pathway controlling plant mycorrhizal symbiosis

Yanhong Zhou[1,2], Shibei Ge[1], Lijuan Jin[1], Kaiqian Yao[1], Yu Wang[1], Xiaodan Wu[3], Jie Zhou[1], Xiaojian Xia[1], Kai Shi[1],Christine H. Foyer[4★] and Jingquan Yu[1,2★]

[1]Department of Horticulture, Zijingang Campus, Zhejiang University, 866 Yuhangtang Road, Hangzhou, 310058, P.R. China.

[2]Key Laboratory of Horticultural Plants Growth and Development, Agricultural Ministry of China, Yuhangtang Road 866, Hangzhou, 310058, P.R. China.

[3]Analysis Center of Agrobiology and Environmental Science, Zhejiang University, Yuhangtang Road 866, Hangzhou, 310058, P.R. China.

[4]Centre for Plant Sciences, Faculty of Biology, University of Leeds, Leeds, LS2 9JT, UK

★Author for correspondence:

Christine H. Foyer

Tel: +44 (1)133 431421

Email: C.Foyer@leeds.ac.uk

Jingquan Yu

Tel:+86 8898 2381

Email: jqyu@zju.edu.cn

Summary

- Rising atmospheric carbon dioxide concentrations (eCO_2) promote symbiosis between roots and arbuscular mycorrhizal fungi (AMF), modifying plant nutrient acquisition and cycling of carbon, nitrogen and phosphate. However, the biological mechanisms by which plants transmit aerial eCO_2 cues to roots, to alter the symbiotic associations remain unknown.
- We used a range of interdisciplinaryapproaches, including gene silencing, grafting, transmission electron microscopy, LC–MS/MS, biochemical methodologies and gene transcript analysis to explore the complexities of environmental signal transmission from the point of perception in the leaves at the apex to the roots.
- Here we show that eCO_2 triggers apoplastic H_2O_2-dependent auxin production in tomato shoots followed by systemic signaling that results in strigolactone biosynthesis in the roots. This redox-auxin-strigolactone systemic signaling cascade facilitates eCO_2-induced AMF symbiosis and phosphate utilization.
- Our results challenge the current paradigm of eCO_2 effects on AMF and provide new insights into potential targets for manipulation of AMF symbiosis for high nutrient utilization under future climate change scenarios.

Key words: apoplastic H_2O_2, arbuscular mycorrhizal fungi (AMF), auxin, elevated CO_2, phosphate uptake, strigolactone, systematic signalling, tomato (Solanum lycopersicum)

Introduction

Symbiosis between plants and arbuscular mycorrhizal fungi (AMF) facilitates efficient utilization of nutrients and alters carbon (C), nitrogen (N) and phosphate (P) cycling in terrestrial ecosystems (van der Heijden et al., 1998; Smith & Smith, 2011). Beneficial symbioses are predicted to play an increasingly important role in plant adaptation to projected increases in atmospheric CO_2 levels, particularly as essential nutrients become exhausted (Heimann & Reichstein, 2008). AMF development is sustained by sugars and lipids supplied by the roots (Kiers et al., 2011; Jiang et al., 2017; Luginbuehl et al., 2017), a process that is regulated by phytohormones such as auxin and strigolactones (SLs) and nutrient availability (Akiyama et al., 2005; Benjamins et al., 2008; Pozo et al., 2015; Lanfranco et al., 2018). For example, SLs trigger fungal pre-symbiotic development, while auxin signaling promotes AM formation (Gutjahr, 2014; Guillotin et al., 2017). Phosphate-deprived plants secrete SLs to initiate the establishment of symbiotic relationships with AMF (Akiyama et al., 2005; Bucher, 2007). The AM symbiosis on roots is promoted by elevated atmospheric CO_2 (eCO_2) (Drigo et al., 2010; Terrer et al., 2016). To date, eCO_2 effects on mycorrhizal symbiosis have been explained largely in terms of an increased flux of photo-assimilates to roots (Roth & Paszkowski, 2017). However, increases in photoassimilate availability are predominantly used for root growth leading to increased root/shoot ratios as nutrients such as nitrogen and phosphorus become limiting, and there is little change in the accumulation of carbohydrates in the roots (Jauregui et al., 2015). Moreover, eCO_2 exerts many local and systematic effects on plant biology, including changes in redox homeostasis, hormone signaling, root development and defense responses (Munné-Bosch et al., 2013; Jin et al., 2015; Shi et al., 2015; Mhamdi & Noctor, 2016). Such observations suggest the probable existence

of an as yet uncovered and largely carbohydrate-independent systemic signaling pathway that underpins plant responses to eCO_2. Here we address the key question of how plants transmit eCO_2 signals systematically from the shoot to the roots in order to induce appropriate responses including effects on plant-mycorrhizal symbioses and associated nutrient uptake.

Material and methods

Plant material, plant growth and growth conditions

Wild-type tomato (Solanum lycopersicum L. cv. Ailsa Craig), a mutant in a cyclophilin A called diageotropica (dgt) in the Ailsa Craig background and transgenic tomato DR5:GUS lines in the Ailsa Craig and dgt backgrounds (Dubrovsky et al., 2008) were obtained from M. G Ivanchenko of Oregon University, USA. The dgt mutant plants show a pleiotropic phenotype including lack of geotropism, abnormal xylem structure, lack of lateral roots (LRs), and higher shoot-to-root ratios with abnormal auxin fluxes (Lavy et al., 2012). The AMF used in the following studies was an isolate of Rhizophagus irregularis, which was propagated in pot cultures with Zea mays L.

To generate the RBOH1RNAi construct, a 318-bp specific DNA fragment of SlRBOH1 was amplified with the specific primers SlRBOH1-F (5′-GGCCatttaaatggatccCGTTCAGCTCTCATTACC-3′) and SlRBOH1-R (5′-TTggcgcgcctctagaCCGAAGATAGATGTGTGT-3′), which had been tailed with BamHI/XbaI and SwaI/AscI restriction sites at the 5′ end, respectively. The amplified products were digested with BamHI/XbaI and SwaI/AscI and ligated into the pFGC5941 vector at the BamHI/XbaI restriction site in the sense orientation and at the SwaI/AscI restriction site in the antisense orientation. The resulting plasmid was

transformed into Agrobacterium tumefaciens strain EHA105 and transformed into cotyledon of tomato (cv. Ailsa Craig) as described (Fillatti et al., 1987). Transgenic plants were identified by resistance to the herbicide Basta and then characterized by RT-qPCR.

To determine the role of SL biosynthesis and SL signaling in eCO_2-induced AMF development and P uptake, we used virus-induced gene silencing (VIGS) to suppress the transcript of CCD7, CCD8, MAX1 and MAX2 with the tobacco rattle virus (TRV)-based vectors (pTRV1/2) (Liu et al., 2002). The cDNA fragment of CCD7, CCD8, MAX1 and MAX2 was PCR-amplified using the gene-specific primers listed in Table S1. The amplified fragment was digested with EcoRI and XbaI, BamHI and XbaI, respectively, and ligated into the corresponding sites of the pTRV2 vector. Empty pTRV2 vector was used as a control. All constructs were confirmed by sequencing and subsequently transformed into Agrobacterium tumefaciens strain GV3101. VIGS was performed by infiltration of germinated seeds, followed by infiltration into the fully expanded cotyledons of 15-d-old tomato seedlings with A. tumefaciens harboring a mixture of pTRV1 and pTRV2-target gene in a 1:1 ratio. Plants were grown at 23/21 ^{o}C (day/night) in a growth chamber with a 12 h day length for 30 d until control pTRV-PDS plants (silencing of the gene encoding phytoene desaturase) showed strong bleaching (Ekengren et al., 2003). qRT-PCR analysis was performed to evaluate gene silencing efficiency.

To determine the respective role of RBOH1 expression in the shoot and roots in the AM fungal growth, shoots of wild type (WT) and RBOH1-RNAi (rboh) plants at 3-leaf stage were self-grafted or reciprocally grafted onto roots of WT and rboh, respectively, which resulted in four combinations: WT/WT, rboh/rboh, rboh/WT and WT/ rboh. Similarly, shoots of WT and dgt plants at 3-leaf stage were self-grafted or

reciprocally grafted onto roots of WT and dgt roots, respectively, which resulted in four combinations: WT/WT, dgt/dgt, dgt/WT and WT/dgt. After adaptation under dark for 3 d, the grafted plants were transferred to growth chambers with the following environmental conditions: 12-h photoperiod, temperature of 25/20 °C (day/night) and photosynthetic photon flux density (PPFD) of 600 μmol photons m^{-2} s^{-1}.

Tomato plants at 5-leaf stage were transplanted to pots (150 ml) filled with a sterilized soil/quartz sand/vermiculite mixture (1/1/1) or to pots containing the same mixture inoculated with Rhizophagus irregularis at a dose of 800 spores per plant or grown hydroponically in Hoagland's nutrient solution (Hoagland et al., 1950). The content of extractable soil P was 8 mg kg^{-1}. Plants were allowed to grow under two atmospheric CO_2 conditions (aCO_2 at 380 ppmv and eCO_2 at 800 ppmv) in controlled growth chambers. CO_2 was supplied to the growth chambers using compressed CO_2 gas and automatically controlled at ±10 ppmv. For the pot plants, seedlings were supplied with Hoagland's nutrient solution containing 1 mM KH_2PO_4 or Hoagland's nutrient solution without KH_2PO_4 but with the addition of 1mM KCl. Plants were watered daily with distilled water and fertilized with Hoagland nutrition solution every 2 d. For the hydroponically-grown plants, seedlings were exposed to P sufficient (1 mM KH_2PO_4) or P deficient (0.05mM KH_2PO_4 with the addition of 0.95 mM KCl) conditions. For the AMF inoculation, Rhizophagus irregularis inoculum was sandwiched between the bottom (100 g) and top (50 g) layers of the substrate in each pot. The plants were placed in a controlled environment chamber with a day/night temperature of 25/20 °C and a 12 h photoperiod. The photosynthetic photon flux density (PPFD) was 600 μmol m^{-2} s^{-1} s. For biomass and P content measurements, leaves, stems and roots were harvested, dried at 80 °C for 3 d before analysis.

Histological analyses and microscopy

To detect mycorrhizal colonization, root segments were rinsed by water and incubated in 10% (w/v) KOH heated to 90 ^{o}C for 1 h and then rinsed with water prior to acidification with 2% HCl solution for 5 min. The root samples were then stained with 0.05% Trypan Blue, heated to 90 ^{o}C for 30 min and decolored 1 day by Lactic acid and glycerin (1:1, v/v). Then the root samples were observed under a Leica DM4000B microscope (Leica Microsystems, Germany) for mycorrhizal fungal colonization. A total of ca. 300 root/gridline intersects were recorded to assess the colonization level according to gridline intersect method described by Giovanetti and Mosse (1980).

To determine the auxin signaling intensity, two transgenic tomato DR5:GUS lines with Ailsa Craig or dgt backgrounds (Ekengren et al., 2003) were used directly or as rootstock with shoots of RBOH1-RNAi and dgt plants as scion, respectively. GUS staining was performed as described previously (Ivanchenko et al., 2006). Root samples were analyzed under a Leica DM4000B microscope (Leica Microsystems, Wetzlar, Germany) with differential interference contact (DIC) optics. H_2O_2 in apex leaves was visualized at the subcellular level using $CeCl_3$ for localization, as described previously (Thordal-Christensen et al., 1997; Xia et al., 2009).

Pi and H_2O_2 quantification

Metabolism was arrested in dried leaves, stems and root samples (0.1 g by grindingin 2 ml 4:1 mixtures (v/v) of 65% nitric and 70% perchloric acids. The homogenates were filtrated and diluted with distilled water. The pH value was adjusted to 7~8. Pi measurements were conducted as previously described (Delhaize and Randall, 1995). H_2O_2 was extracted from leaf tissue and measured as described previously (Xia et al., 2009).

Expression analysis by qRT-PCR

Gene expression analyses were done by qRT-PCR as previously described (Wang et al., 2016), with primers listed in Table S2.

Measurement of hormones levels

For the analysis of IAA, the developing leaves at the apex were used. IAA extraction and quantification were performed as described previously (Guo et al., 2016). For the determination of SLsin the roots, 0.5 g of roots was blended in a blender at top speed for 1 min in 40% acetone (1:5, w/v). After centrifugation for 5 min, SLs in the residues were extracted with 50% acetone (1:5, w/v). The acetone was evaporated under reduced pressure at 35 ºC. Root extracts were dissolved in methanol:water (1:1, v/v). SLs were detected using an Agilent 6460 triple quadrupole mass spectrometer (Agilent Technologies, USA) equipped with an electrospray ionization (ESI) source, operated in positive mode. HPLC separation was performed on a Zorbax SB C18 column (150×2.1 mm, 3.5 μm). The mobile phases consisted of formic acid:water (1:100, v/v; solution A) and acetonitrile (solution B). The gradient program was as follows: 20–48% B in 3min, 48–50% B in 2 min,50–53% B in 1min, 53–65% B in 1min, 65–95% B in 0.5min, 95% B for 3.5 min. The flow rate was set at 0.3 ml min^{-1}. The SLs were detected in multiple reaction monitoring (MRM) mode (Koltai et al., 2011). SLs contents were expressed as the relative content with peak area for plants under aCO_2 as 1.

Seed germination

Germination assays were performed using Orobanche ramose seeds as reported previously with minor modifications (Matusova et al., 2005). Seeds of Orobanche ramose were preconditioned for 14 days at 21°C before the seeds became responsive to germination stimulants. Aliquots (50 μl) of 50% acetone extracts of tomato roots were added to duplicate 1-cm discs bearing approximately 50 preconditioned seeds

each. The synthetic germination stimulant GR24 (10^{-6} mM) and demineralized water were included as positive and negative controls in each bioassay. After 7 days, the germinated and ungerminated seeds were counted using a binocular microscope. Seeds were considered germinated when the radicle had protruded through the seed coat.

Statistical analysis

A completely randomized block design with at least three independent replicates was used in each experiment. Each replicate involved 15~20 plants. Data were statistically analyzed by analysis of variance (ANOVA). The significance of treatment differences was analyzed using Tukey's test ($P < 0.05$).

Results

eCO_2 induces strigolactone biosynthesis and AMF symbiosis

To gain a better understanding of how eCO_2 alters the plant-AMF symbiosis and associated P utilization efficiency, we firstly compared biomass accumulation, organ P content and AMF development in tomato plants grown in a soil/quartz sand/vermiculite mixture (1/1/1) in the absence or presence of a P supply and inoculation with the AMF Rhizophagus irregularis under ambient CO_2 (aCO_2, 380 ppmv) or eCO_2 (800 ppmv) conditions for 28 d. P starvation-induced decreases in plant biomass accumulation, tissue P concentrations and total plant P accumulation were greatly attenuated by inoculation with AMF and by eCO_2 (Figs 1a, S1a,b). Conversely, AMF development was suppressed by adequate P supply. Growth under eCO_2 significantly improved AMF development on the roots, especially under P starvation conditions, as shown by increased AMF colonization (Figs 1b, S1c). Significantly, the levels of transcripts encoding the SL synthesis enzymes,

CAROTENOID CLEAVAGE DIOXYGENASE 7 (CCD7), CCD8 and MORE AXILLARY BRANCHING 1 (MAX1), and MAX2, which are required for SL signaling in the roots, were induced by eCO_2, especially under P starvation and in the presence of AMF (Figs 1c, S2a). Moreover, the increase in the levels of CCD7, CCD8, MAX1 and MAX2 transcripts was accompanied by a large increase in the accumulation of orobanchol, didehydro-orobanchol and solanacol, which are the three principal SLs in the roots of tomato plants measured under eCO_2 conditions, regardless of the P level or the presence of AMF (Fig. S2b). Concomitant with these changes, growth under eCO_2 resulted in a higher abundance of transcripts encoding several phosphate transporters (PT1, PT2, PT3, PT4 and PT5) (Fig. S3). This was especially marked under conditions of P starvation and in the presence of AMF. These results show that eCO_2-promoted AMF colonization and P uptake are linked to enhanced SL biosynthesis and signaling in roots.

Requirement for leaf RBOH1 expression in the systemic induction of auxin signaling by eCO_2

Apoplastic H_2O_2 production can trigger auxin production, which hence has a potential role in the regulation of AMF growth (Etemadi et al., 2014; Chen et al., 2016). We, therefore, determined the local and systemic impacts of eCO_2 on H_2O_2 homeostasis and the levels of auxin in the apex, together with auxin signaling in the roots in plants grown either with sufficient P supply or under P deficient conditions. The levels of RESPIRATORY BURST OXIDASE HOMOLOG1 (RBOH1) transcripts encoding NADPH oxidase, which is involved in apoplastic H_2O_2 generation, increased in the apex leaves of plants grown under eCO_2 (Fig. 2a),. Concurrently, the levels of FLAVIN MONOOXYGENASE (FZY) mRNAs that encode an enzyme catalyzing a

rate-limiting step in auxin biosynthesis, the accumulation of H_2O_2 in the apoplast and the levels of indole-3-acetic acid (IAA) increased (Figs. 2b,-c, Fig. S4a,b). These eCO_2-dependent increases were particularly marked under conditions of P deficiency, and were observed within one day of exposure to eCO_2. Histochemical analysis of GUS-activity revealed that the auxin-responsive reporter gene DR5 was more highly expressed in root tips of plants grown under eCO_2 (Fig 2d). Similarly, the abundance of IAA15 transcripts was increased in roots under eCO_2, especially under conditions of P starvation (Fig. S4c). Taken together, these results show that eCO_2 not only induces local changes in redox and auxin homeostasis of the apex, but also leads to enhanced auxin signaling in the roots as a result of greater polar auxin transport (PAT) from the shoots.Interestingly, the eCO_2-induced accumulation of IAA was observed in WT plants but absent from the apex of the RBOH1-RNAi (rboh) plants, regardless of P level (Fig. S5a). When rboh shoots were grafted onto the roots of wild type (WT) plants (rboh/WT), eCO_2-induced accumulation of IAA and DR5 in the roots were attenuated (Fig. S5b,c). Moreover, exogenous application of H_2O_2 to the leaves resulted in an increase in the accumulation of IAA in the apex, a concentration of 100 µM H_2O_2 being the most effective in stimulating IAA accumulation (Fig. S5d).

By using reciprocal grafting with WT and rboh1 as scion (S) or rootstock (R), respectively, we obtained four graft combinations (S/R), WT/WT, WT/rboh, rboh/WT and rboh/rboh. When these plants were grown in the presence of AMF under P deficient conditions, rboh/WT and rboh/rboh plants showed less IAA accumulation in the apex, with a lower tissue P concentration and plant dry matter and less overall P accumulation in the plants (Figs 2e, S6a-c). While eCO_2 induced significant increases in the accumulation of IAA in the apex, as well as increases in plant biomass and P accumulation in the WT/WT plants and to a lesser degree in WT/rboh plants, these

effects were either not observed or they were attenuated in the rboh/WT and rboh/rboh plants (Fig. S6a-c). Moreover, AMF colonization rates were decreased (Figs. 2f, S7a). In addition, the eCO_2-induced increases in AMF colonization and transcript of PT4 and PT5 as well as in P accumulation were attenuated in the roots of rboh/WT and rboh/rboh plants (Figs 2e,f, S6c, S7). These findings show that expression of RBOH1 in the shoots plays a critical role in eCO_2-induced IAA biosynthesis and in systemic signaling leading to enhanced AMF symbiosis and P utilization, as well as whole plant growth under conditions of P deficiency.

Dependency of strigolactone biosynthesis on auxin signaling in leaves

Auxin perception is required for arbuscule development in the mycorrhizal symbiosis (Etemadi et al., 2014). To determine whether eCO_2-dependent IAA biosynthesis in the apex is required for systemic signaling leading to greater AMF symbiosis and P utilization, we conducted a further series of grafting experiments using WT and an auxin-resistant diageotropica (dgt) mutant that has impaired PAT (Ivanchenko et al., 2015) as rootstock or scion respectively. Under eCO_2 conditions, the WT/WT plants had the highest biomass, tissue P concentrations and greatest overall P accumulation, as well as the highest levels of AMF colonization in the roots, followed by the WT/dgt, dgt/WT and dgt/dgt plants, in the absence of P supply (Figs 3a,b, S8, S9a). The effects of eCO_2 on biomass accumulation, P concentration and accumulation, AMF colonization and the transcript of PT4 and PT5 were less marked in the WT/dgt plants than the WT/WT controls. Crucially, eCO_2 had little effect on the dry biomass, tissue P concentration and P accumulation, AMF colonization and the transcript of PT4 and PT5 in the dgt/WT and dgt/dgt plants (Figs. 3a,b, S8, S9). Taken together, these results demonstrate that auxin signaling in the shoots plays a vital role in

eCO_2-induced AMF growth and P uptake.

DR5-GUS staining studies showed that while DR5 accumulation was only slightly induced in the roots as a result of P starvation, it was greatly increased in plants exposed to eCO_2 (Fig. S10a). However, the eCO_2-dependent induction in DR5 accumulation was abolished in plants with dgt as scion. In contrast, DR5 accumulation was induced in the roots of WT/dgt plants under eCO_2 conditions but to a lesser degree, presumable because the mobility of DGT protein could remedy DGT deficiency, at least in part, in the dgt roots (Spiegelman et al., 2014) (Fig. S10b). Therefore, eCO_2-induced increase in auxin biosynthesis in the leaves and associated polar auxin transport (PAT) contributes the systemic induction of auxin signaling in the roots, AMF symbiosis and P utilization.

Given eCO_2-induced SL signaling and its role in AMF symbiosis in the roots (Akiyama et al., 2005) (Fig. 1), we next examined whether SL biosynthesis is subject to the regulation of auxin signaling from the leaves. By using WT or dgt as scion, respectively, we observed decreased levels of CCD7, CCD8, MAX1 and MAX2 transcripts and a decreased accumulation of orobanchol, didehydro-orobanchol and solanacol in the roots of the dgt/WT plants compared to WT/WT plants (Figs 3c, S11). Crucially, eCO_2 failed to stimulate an increase in the expression of CCD7, CCD8, MAX1 and MAX2, or the accumulation of orobanchol, didehydro-orobanchol and solanacol in the roots of the dgt/WT plants. Taken together, these results indicate that eCO_2 induces not only local changes in the redox-dependent auxin homeostasis in the apex, but also the induction of SL biosynthesis and expression of PT genes in the roots, as a consequence of auxin-dependent systemic signaling.

Strigolactone signaling plays a role in eCO_2-promoted AMF symbiosis and P

utilization

SLs are important signals that activate the fungal partner in the plant/AMF symbiosis, particularly with respect to the stimulation of hyphal branching (Akiyama et al., 2005; Besserer et al., 2006). To determine whether eCO_2-induced SL synthesis and signaling play a role in eCO_2-induced AMF colonization and P utilization, we silenced CCD7 (pTRV-CCD7), CCD8 (pTRV-CCD8), MAX1 (pTRV-MAX1), and MAX2 (pTRV-MAX2) by virus-induced gene silencing (VIGS). This resulted in a reduction of the transcripts by ca. 80% (Fig. S12a). Consistent with the role of SL in shoot and root branching (Gomez-Roldan et al., 2005), silencing these genes promoted bud outgrowth with increased numbers of later branches observed under standard growth conditions (Fig. S12b). In agreement with this observation, root extracts from the pTRV-CCD7, pTRV-CCD8 and pTRV-MAX1 plants showed a decreased accumulation of the three SLs and stimulation of germination of Orobanche ramose seeds compared to the empty vector control plants (pTRV). In comparison, root extracts from the pTRV-MAX2 plants showed similar accumulation of the three SLs stimulation and caused a similar degree of germination to the pTRV controls (Fig. S12c). These findings confirm that SL synthesis was significantly suppressed in the roots of the pTRV-CCD7, pTRV-CCD8 and pTRV-MAX1 plants but not in the SL signaling silenced plants pTRV-MAX2. Importantly, the pTRV-CCD7, pTRV-CCD8, pTRV-MAX1 and pTRV-MAX2 plants showed decreased plant growth, lower levels of PT1, PT2, PT3, PT4 and PT5 transcripts, and less P accumulation in response to P starvation compared to the pTRV controls under both aCO_2 and eCO_2 conditions (Figs 4a,c, S13a-c). Crucially, eCO_2-induced stimulation of plant growth, AMF colonization and development, the levels of PT1, PT2, PT3, PT4 and PT5 transcripts and P accumulation were compromised in the pTRV-CCD7, pTRV-CCD8, pTRV-MAX1 and

pTRV-MAX2 plants (Figs 4, S13). However, no significant differences were found in the pTRV-CCD7, pTRV-CCD8, pTRV-MAX1 and pTRV-MAX2 plants in terms of biomass accumulation, P concentration, P accumulation, AMF colonization rate, indicating that both SL biosynthesis and signaling are involved in the eCO_2-induced regulation of AMF colonization and P uptake.

Discussion

The most common mechanism by which higher plants optimize soil P uptake in response to eCO_2, is through AM symbiosis (Terrer et al., 2016). In a synthesis of 135 published studies, Compant et al. (2010) reportedthat eCO_2 generally had a positive influence on AMF colonization. However, the effects of eCO_2 and P supply on the AMF varies with the host plant type, AMF species andlimate factors, as well as soil biology and chemistry (Jakobsen et al. 2016). Here, we report that growth under eCO_2 significantly improved AMF development on tomato roots, especially under P starvation conditions (Figs 1b, S1c). Notably, enhanced AM symbiosis was followed by increased P accumulation and plant growth (Figs 1a, S1a,b). taken together these findings suggest that AM symbiosis will become increasingly important for plants in the future, as the atmospheric CO_2continue to increase placing increasing demands on soil P availability.

To date, the mechanisms by which plants transmit eCO_2 signals systematically from the shoots to the roots have remained unclear. The simplest scenario would be that with increased CO_2 fixation, more C would be available for transfer to AMF and hence the percentage of colonization would increase. The data presented here reveals the existence of a previously unrecognized systemic redox-hormone signaling pathway and provides a critical new insights into the mechanisms underpinning

eCO_2-induced symbiosis. In the conceptual framework presented here (Fig. 5), eCO_2 triggers the apoplastic H_2O_2 dependent production of auxin in the tomato shoots followed by systemic induction of auxin signaling and resultant strigolactone biosynthesis in the tomato roots. In the absence of AMF, this signaling cascade may alter root system architecture (RSA) to enhance phosphate absorption as both auxin and SLs participate in the regulation of root system architecture (Ham et al. 2018). In the presence of AMF in the soil, this redox-auxin-strigolctone systemic signaling cascade can be used to facilitate mycorrhizal symbiosis and subsequent increased phosphate uptake from the soil. Moreover, our observations demonstrate that this signaling cascade is required for AMF symbiosis in response to eCO_2 regardless of the presence of enhanced carbohydrate availability.

ROS play a critical role in plant growth, development and responses to environmental stimuli (Xia et al., 2015). However, up to now it has remained unknown whether they are involved in eCO_2-induced AM symbiosis and P uptake. Here, we demonstrate that leaf RBOH1 expression is essential for eCO_2-induced AM symbiosis and associated P uptake. Growth under eCO_2 increased the levels of RBOH1 transcripts and the accumulation of H_2O_2 in the apoplast. Conversely, suppressed expression of RBOH1 in the shoot (rboh/WT) compromised eCO_2-induced AM symbiosis and P uptake (Figs 2, S6c, S7). Hence, eCO_2alters cellular redox homeostasis as discussed previously (Mhamdi and Noctor, 2018). In addition, RBOH-mediated ROS production facilitates lateral root emergence in Arabidopsis (Shi et al., 2015; Orman-Ligeza et al., 2016). The data presented here demonstrates that RBOH1 expression in the roots of WT/rboh1 plants had little effect on AM symbiosis and P uptake in response to changes in the concentration of atmospheric CO_2 compared to rboh/WT plants (Figs 2e,f, S6c, S7). Therefore,

eCO_2 promote AM symbiosis by triggering ROS production in the shoots, rather by than in the roots.

While auxin signaling is known to promoteAM development (Etemadi et al., 2014; Chen et al., 2016), it has remainedunclear whether auxin participates in eCO_2-induced AM symbiosis. The data presented here show that there was an increase in RBOH1-dependent IAA accumulation in response to eCO_2, with the induction of transcripts encoding the auxin biosynthesis gene FZY (Fig. S4a). Crucially, plants with impaired PAT (dgt/WT and dgt/dgt) showed a compromised response to eCO_2 in term of auxin signaling (DR5 accumulation), AM symbiosis and P uptake, suggesting that auxin signaling is responsible for eCO_2-induced AM symbiosis (Figs 3a,b, S8-10). In addition, the dta presented her show that auxin biosynthesis was subject to redox regulation. Suppression of RBOH1 transcripts attenuated eCO_2-induced accumulation of IAA in the apex of rboh/WT plants (Fig. S6a). These results provide convincing evidences that redox signaling acts as a second messenger of auxin signaling in promoting AMF symbiosis and P utilization.

Auxin is involved in the regulation of SL biosynthesis in roots (Koltai, 2015). The auxin deficient bushy mutant of pea showed decreased expression of the SL biosynthesis gene CCD8 and reduction in SL biosynthesis resulting in low AM colonization (Foo, 2013). Similarly, the application of IAA increased root SL accumulation, while the application of an auxin transport inhibitor decreased SL accumulation in the roots (Yoneyama et al., 2015). Consistent with these fimdings, we show here that the roots of the dgt/WT plants had decreased levels of CCD7, CCD8, MAX1 and MAX2 transcripts with a lower accumulation of orobanchol, didehydro-orobanchol and solanacol compared to WT/WT plants (Fig. 3c, S11). Moreover, eCO_2 failed to stimulate an increase in the expression of these genes or the

accumulation of these SLs in the roots of the dgt/WT plants. Taken together, these results collectively indicate that eCO_2 induces a systemic redox-auxin-SL signaling cascade that promotes AMF symbiosis and P utilization.

SLs have well known roles in seed germination, plant architecture, stress responses and AM symbiosis (Akiyama et al., 2005; Besserer et al., 2006; Mostofa et al., 2018). Consistent with previous studies, the data presented here show that the CCD7, CCD8, MAX1 and MAX2-silenced plants had low AM colonization and P uptake (Figs. 4a,b, S13b,d). Importantly, silencing these genes also compromised eCO_2-induced AM colonization, decreased the levels of PT transcripts and P uptake, suggesting that SL biosynthesis and signaling are pivotal to eCO_2-induced AM colonization and P uptake. Up to now, both induced or suppressed expressionof PT genes has beenobserved during AM symbiosis in different plant species. This has been mostly attributed to differences in parameters such as AM or plant species, growth stage, culture system and experimental conditions applied (Nagy et al., 2005; Balestrini et al., 2006; Fiorilli et al., 2009; Smith et al., 2011). In tomato, the expression of PT1, PT3 and PT4 was differentially induced by mycorrhizal inoculum (Xu et al., 2007). In addition, mutation of PT4 resulted in decreased P accumulation, with low plant biomass accumulation in the absence of mycorrhiza inoculum, suggesting that PT4 is not only responsive to AMF but that it is also required for appropriate P status. In our studies, we show that eCO_2 increased the induction of expression of the PT genes and that this was particularly significant for the PT4 transcripts in the presence of AMF. These findings suggest that PT4 is pivotal in eCO_2-induced and AMF-mediated P accumulation (Fig. S3). This dataset also raised the possibility of involvement of SLs and AMF in the regulation of PT gene expression through interactions with other P-related physiological processes.

In support of this conclusion the max2-1 mutants displayed a lower induction of the expression of several phosphate-starvation response and phosphate-transporter genes (Mayzlish-Gati et al., 2012).

In conclusion, the data presented here demonstrate the presence of a previously unrecognized redox-auxin-strigolctone systemic signaling cascade that facilitates mycorrhizal symbiosis and subsequent phosphate uptake in plants from soils. The findings have the following important implications for our current understanding plant responses to climate change. Firstly, plants have evolved a systemic signaling cascade that allows adaption to climate change. This strategy is especially important for adaptations to increased atmospheric CO_2 levels and decreased P availability in terrestrial ecosystems, in which plants rely largely on AMF for mineral nutrients. Secondary, our studies highlight the importance of incorporating considerations of AMF-dependent effects on C, water and nutrient cycles in assessments of eCO_2 impacts in ecosystems, as well as in future climate change scenarios because eCO_2-induced AMF not only have a major impact on plant variability and productivity through plant-soil feedback processes (van der Heijden et al., 1998; Clemmensen et al., 2013; Teste et al.,2017), but also on the biodiversity of soil microbial communities and associated turnover of C, N and P in soil (Compant et al., 2010; Cheng et al.,2012). Finally, our studies illustrate the potential for increasing nutrient utilization efficiency by targeting the components involved in the systemic signaling pathway described here, especially for improvement of crop productivity on marginal or infertile soils. Such considerations could also serve to reduce environmental pollution arising from high dose fertilization that is currently used in agricultural production systems.

Acknowledgements

M. G. Ivanchenko and Tomato Genetics Resource Center at the California University for providing tomato seeds; G. Feng and X.L. Li for providing Rhizophagus irregularis isolate and their advice; J. Hong for the electron microscopy observation. Thanks are also due to Prof. S.J. Hu for the valuable discussion during the study. This work was supported by grants from the National Natural Science Foundation of China (31825023, 31430076), the Modern Agro-industry Technology Research System of China (CARS-25-02A), and the Biotechnology and Biological Sciences Research Council (BBSRC) UK (BB/M009130/1).

Author contributions

Y.Z., S.G., L.J., K.Y. and Y.W. performed the experiments; X.W. carried out mass spectrometry analysis; X.X., J.Z. and K.S. provided technical and intellectual support; C.F. and J.Y conceived the project, designed the experiments, analyzed the data and wrote the manuscript with the help of all authors.

References

Akiyama K, Matsuzaki K, Hayashi H. 2005. Plant sesquiterpenes induce hyphal branching in arbuscular mycorrhizal fungi. Nature **435**: 824–827.

Balestrini R, Lanfranco L. 2006. Fungal and plant gene expression in arbuscular mycorrhizal symbiosis. Mycorrhiza **16**: 509-524.

Benjamins R, Scheres B. 2008. Auxin: The looping star in plant development. Ann Rev Plant Biol **59**: 443–465

Besserer A, Puech-Pagès V, Kiefer P, Gomez-Roldan V, Jauneau A, Roy S, Portais JC, Roux C, Bécard G, Séjalon-Delmas N. 2006. Strigolactones stimulate

arbuscular mycorrhizal fungi by activating mitochondria. PLoS Biol **4**: 1239–1247.

Chen XJ, Xia XJ, Guo X, Zhou YH, Shi K, Zhou J, Yu JQ. 2016. Apoplastic H_2O_2 plays a critical role in axillary bud outgrowth by altering auxin and cytokinin homeostasis in tomato plants. New Phytol **211**: 1266–1278.

Cheng L, Booker FL, Tu C, Burkey KO, Zhou L, Shew HD, Rufty TW, Hu S. 2012. Arbuscular mycorrhizal fungi increase organic carbon decomposition under elevated CO_2. Science **337**: 1084–1087.

Clemmensen KE, Bahr A, Ovaskainen O, Dahlberg A, Ekblad A, Wallander H, Stenlid J, Finlay RD, Wardle DA, Lindahl BD. 2013. Roots and associated fungi drive long-term carbon sequestration in boreal forest. Science **339**: 1615–1618.

Compant S, van der Heijden MG, Sessitsch A. 2010. Climate change effects on beneficial plant-microorganism interactions. FEMS Mircrobiol Ecol **73**:197–214.

Delhaize E, Randall PJ. 1995. Characterization of a phosphate-accumulator mutant of Arabidopsis thaliana. Plant Physiol **107**: 207–213.

Drigo B, Pijl AS, Duyts H, Kielak A, Gamper HA, Houtekamer MJ, Boschker HTS, Bodelier PLE, Whiteley AS, van Veen JA, et al. 2010. Shifting carbon flow from roots into associated microbial communities in response to elevated atmospheric CO_2. Proc Natl Acad Sci **107**: 10938–10942.

Dubrovsky JG, Sauer M, Napsucialy-Mendivil S, Ivanchenko MG, Friml J, Shishkova S, Celenza J, Benková E. 2008. Auxin acts as a local morphogenetic trigger to specify lateral root founder cells. Proc Natl Acad Sci **105**: 8790–8794.

Ekengren SK, Liu Y, Schiff M, Dinesh-Kumar SP, Martin GB. 2003. Two MAPK cascades, NPR1, and TGA transcription factors play a role in Pto-mediated disease resistance in tomato. Plant J **36**: 905–917.

Etemadi M, Gutjahr C, Couzigou JM, Zouine M, Lauressergues D, Timmers A,

Audran C, Bouzayen M, Bécard G, Combier JP. 2014. Auxin perception is required for arbuscule development in arbuscular mycorrhizal symbiosis. Plant Physiol **166**:281–292.

Fiorilli V, Catoni M, Miozzi L, Novero M, Accotto GP, Lanfranco L. 2009. Global and cell-type gene expression profiles in tomato plants colonized by an arbuscular mycorrhizal fungus. New Phytologist **84**: 975-987.

Fillatti JJ, Kiser J, Rose R, Comai L. 1987. Efficient transfer of a glyphosate tolerance gene into tomato using a binary Agrobacterium tumefaciens vector. Nat Biotechnol **5**:726–730.

Foo E. 2013. Auxin influences strigolactones in pea mycorrhizal symbiosis. J Plant Physiol **170**: 523-528.

Giovannetti M, Mosse B. 1980. An evaluation of techniques for measuring vesicular arbuscular mycorrhizal infection in roots. New Phytologist **84**: 489–500.

Gomez-Roldan V, Fermas S, Brewer PB, Puech-Pagès V, Dun EA, Pillot JP, Letisse F, Matusova R, Danoun S, Portais JC, et al. 2008. Rochange. Strigolactone inhibition of shoot branching. Nature **455**: 189–194.

Guillotin B, Etemadi M, Audran C, Bouzayen M, Becard G, Combier J-P. 2017. Sl-IAA27 regulates strigolactone biosynthesis and mycorrhization in tomato (var. MicroTom). New Phytologist **213**: 1124-1132.

Guo Z, Wang F, Xiang X, Ahammed GJ, Wang M, Onac E, Zhou J, Xia X, Shi K, Yin X, et al. 2016. Systemic induction of photosynthesis via illumination of the shoot apex is mediated sequentially by phytochrome B, auxin and hydrogen peroxide in tomato. Plant Physiol **172:** 1259-1272.

Gutjahr C. 2014. Phytohormone signalling in arbuscular mycorhiza development. Curr Opin Plant Biol **20**: 26-34.

Nagy R, Karandashov V, Chague W, Kalinkevich K, Tamasloukht M, Xu GH, Jakobsen I, Levy AA, Amrhein N, Bucher M. 2005. The characterization of novel mycorrhiza-specific phosphate transporters from Lycopersicon esculentum and Solanum tuberosum uncovers functional redundancy in symbiotic phosphate transport in solanaceous species. Plant Journal **42**(2): 236-250.

Ham B-K, Chen J, Yan Y, Lucas WJ. 2018. Insights into plant phosphate sensing and signaling. Curr Opin Biotech **49**: 1-9.

Heimann M, Reichstein M. 2008. Terrestrial ecosystem carbon dynamics and climate feedbacks. Nature **451**: 289–292.

Herrera-Medina MJ, Steinkellner S, Vierheilig H, Ocampo Bote JA, García Garrido JM. 2007. Abscisic acid determines arbuscule development and functionality in the tomato arbuscular mycorrhiza. New Phytol **175**:554–564.

Hoagland DR, Arnon DI. 1950. The water-culture method for growing plants without soil. Calif Agric Exp Stn Circ **347**: 357–359.

Ivanchenko MG, Coffeen WC, Lomax TL, Dubrovsky JG. 2006. Mutations in the Diageotropica (Dgt) gene uncouple patterned cell division during lateral root initiation from proliferative cell division in the pericycle. Plant J **46**: 436–447.

Ivanchenko MG, Zhu J, Wang B, Medvecká E, Du Y, Azzarello E, Mancuso S, Megraw M, Filichkin S, Dubrovsky JG, et al. 2015. The cyclophilin A DIAGEOTROPICA gene affects auxin transport in both root and shoot to control lateral root formation. Development **142**: 712–721.

Jakobsen I, Smith SE, Smith FA, Watts-Williams SJ, Clausen SS, Grønlund M. 2016. Plant growth responses to elevated atmospheric CO_2 are increased by phosphorus sufficiency but not by arbuscular mycorrhizas. J Exp Bot **67**: 6173–6186.

Jauregui I, Aparicio-Tejo PM, Avila C, Rueda-López M, Aranjuelo I. 2015. Root and shoot performance of Arabidopsis thaliana exposed to elevated CO_2: A physiologic, metabolic and transcriptomic response. J Plant Physiol **189**: 65–76.

Jiang YN, Wang WX, Xie QJ, Liu N, Liu LX, Wang DP, Zhang XW, Yang C, Chen XY, Tang DZ, et al. 2017. Plants transfer lipids to sustain colonization by mutualistic mycorrhizal and parasitic fungi. Science **356**: 1172–1175.

Jin J, Tang C, Sale P. 2015. The impact of elevated carbon dioxide on the phosphorus nutrition of plants: a review. Ann Bot **116**: 987–999.

Kiers ET, Duhamel M, Beesetty Y, Mensah JA, Franken O, Verbruggen E, Fellbaum CR, Kowalchuk GA, Hart MM, Bago A, et al. 2011. Teciprocal tewards dtabilize vooperation in the mycorrhizal symbiosis. Science **333**: 880–882.

Koltai H. 2015. Cellular events of strigolactone signalling and their crosstalk with auxin in roots. J Exp Bot **66**: 4855-4861.

Koltai H, Cohen M, Chesin O, Mayzlish-Gati E, Bécard G, Puech V, Ben Dor B, Resnick N, Wininger S, Kapulnik Y. 2011. Light is a positive regulator of strigolactone levels in tomato roots. J Plant Physiol **168**: 1993–1996.

Lavy M, Prigge MJ, Tigyi K, Estelle M. 2012. The cyclophilin DIAGEOTROPICA has a conserved role in auxin signaling. Development **139:** 1115-1124.

Liu YL, Schiff M, Dinesh-Kumar SP. 2002. Virus-induced gene silencing in tomato. Plant J **31**:777–786.

Luginbuehl LH, Menard GN, Kurup S, Van Erp H, Radhakrishnan GV, Breakspear A, Oldroyd GED, Eastmond PJ. 2017. Fatty acids in arbuscular mycorrhizal fungi are synthesized by the host plant. Science **356**: 1175–1178.

Matusova R, Rani K, Verstappen FW, Franssen MC, Beale MH, Bouwmeester HJ. 2005. The strigolactone germination stimulants of the plant-parasitic Striga

and Orobanche spp. are derived from the carotenoid pathway. Plant Physiol **139**:920–934 .

Mayzlish-Gati E, De-Cuyper C, Goormachtig S, Beeckman T, Vuylsteke M, Brewer PB, Beveridge CA, Yermiyahu U, Kaplan Y, Enzer Y, et al. 2012. Strigolactones are involved in root response to low phosphate conditions in Arabidopsis. Plant Physiol **160**: 1329-1341.

Mhamdi A, Noctor G. 2016. High CO_2 primes plant biotic stress defences through redox-linked pathways. Plant Physiol **172**:929–942.

Mostofa MG, Li W, Nguyen KH, Fujita M, Lam-Son Phan T. 2018. Strigolactones in plant adaptation to abiotic stresses: An emerging avenue of plant research. Plant Cell Environ **41**: 2227-2243.

Munné-Bosch S, Queval G, Foyer CH. 2013. The impact of global change factors on redox signaling underpinning stress tolerance. Plant Physiol **161**:5–19.

Orman-Ligeza B, Parizot B, de Rycke R, Fernandez A, Himschoot E, Van Breusegem F, Bennett MJ, Perilleux C, Beeckman T, Draye X. 2016. RBOH-mediated ROS production facilitates lateral root emergence in Arabidopsis. Development **143**: 3328-3339.

Pozo MJ, López-Ráez JA, Azcón-Aguilar C, García-Garrido JM. 2015. Phytohormones as integrators of environmental signals in the regulation of mycorrhizal symbioses. New Phytol **205**: 1431–1436.

Roth R, Paszkowski U. 2017. Plant carbon nourishment of arbuscular mycorrhizal fungi. Curr Opini Plant Biol **39**: 50–56.

Shi K, Li X, Zhang H, Zhang GQ, Liu YR, Zhou YH, Xia XJ, Chen ZX, Yu JQ. 2015. Guard cell hydrogen peroxide and nitric oxide mediate elevated CO_2-induced stomatal movement in tomato. New Phytol **208**: 342–353.

Smith SE, Jakobsen I, Grønlund M, Smith FA. 2011. Roles of arbuscular mycorrhizas in plant phosphorus nutrition: interactions between pathways of phosphorus uptake in arbuscular mycorrhizal roots have important implications for understanding and manipulating plant phosphorus acquisition. Plant Physiol **156**: 1050–1057.

Smith SE, Smith FA. 2011. Roles of arbuscular mycorrhizas in plant nutrition and growth: new paradigms from cellular to ecosystem scales. Annu Rev Plant Biol **62**: 227–250.

Spiegelman Z, Ham BK, Zhang Z, Toal TW, Brady SM, Zheng Y, Fei Z, Lucas WJ, Wolf S. 2015. A tomato phloem-mobile protein regulates the shoot-to-root ratio by mediating the auxin response in distant organs. Plant J **83**: 853–863.

Terrer C, Vicca S, Hungate BA, Phillips RP, Prentice IC. 2016. Mycorrhizal association as a primary control of the CO_2 fertilization effect. Science **353**:72–74.

Teste FP, Kardol P, Turner BL, Wardle DA, Zemunik G, Renton M, Laliberté E. 2017. Plant-soil feedback and the maintenance of diversity in Mediterranean-climate shrublands. Science **355**: 173–176.

Thordal-Christensen H, Zhang ZG, Wei YD, Collinge DB. 1997. Subcellular localization of H_2O_2 in plants. H_2O_2 accumulation in papillae and hypersensitive response during the barley-powdery mildew interaction. Plant J **11**:1187–1194.

van der Heijden MGA, Klironomos JN, Ursic M, Moutoglis P, Streitwolf-Engel R, Boller T, Wiemken A, Sanders IR. 1998. Mycorrhizal fungal diversity determines plant biodiversity, ecosystem variability and productivity. Nature **396**: 69–72.

Wang F, Guo ZX, Li HZ, Wang MM, Onac E, Zhou J, Xia XJ, Shi K, Yu JQ, Zhou YH. 2016. Phytochrome A and B function antagonistically to regulate cold tolerance via abscisic acid-dependent jasmonate signaling. Plant Physiol **170**:

459-471.

Xia XJ, Wang YJ, Zhou YH, Tao Y, Mao WH, Shi K, Asami T, Chen Z, Yu JQ. 2009. Reactive oxygen species are involved in brassinosteroid- induced stress tolerance in cucumber. Plant Physiol **150**: 801–814.

Xia XJ, Zhou YH, Shi K, Zhou J, Foyer CH, Yu JQ. 2015. Interplay between reactive oxygen species and hormones in the control of plant development and stress tolerance. J Exp Bot **66**:2839-2856.

Xu G-h, Chague V, Melamed-Bessudo C, Kapulnik Y, Jain A, Raghothama KG, Levy AA, Silber A. 2007. Functional characterization of LePT4: a phosphate transporter in tomato with mycorrhiza-enhanced expression. J Exp Bot **58**: 2491-2501.

Yoneyama K, Kisugi T, Xie X, Arakawa R, Ezawa T, Nomura T, Yoneyama K. 2015. Shoot-derived signals other than auxin are involved in systemic regulation of strigolactone production in roots. Planta **241**: 687-698.

Supporting Informaiton

Additional Supporting Information may be found online in the Supporting Informaiton tab for this articile:

Fig. S1 Elevated CO_2 increases biomass accumulation, P concentration and AMF symbiosis.

Fig. S2 CO_2 systemically up-regulates transcript of strigolactone signaling and accumulation in roots.

Fig. S3 CO_2 systemically up-regulates transcript of PT genes in roots.

Fig. S4 CO_2 induced-changes in redox hemostasis and auxin signaling.

Fig. S5 Shoot RBOH1 regulates IAA accumulation and signaling.

Fig. S6 Importance for RBOH1 expression in IAA accumulation, biomass accumulation and P content.

Fig. S7. CO_2-induced AMF colonization and transcript of PT genes were abolished in grafted plants with rboh mutant as scion or rootstock.

Fig. S8 Auxin signaling regulates biomass accumulation and P content in tomato.

Fig. S9. CO_2-induced AMF colonization and transcript of PT genes were abolished in grafted plants with dgt mutant as scion or rootstock.

Fig. S10 CO_2 systemically up-regulates auxin signaling.

Fig. S11 CO_2-induced accumulation of strigolactones was abolished in plants with dgt mutant as scion.

Fig. S12 Silencing efficiency, phenotype of CCD7, CCD8, MAX1 and MAX2-silencing plants and the stimulation effects on the seeds of Orobanche ramose

Fig. S13 Strigolactones mediate CO_2-induced biomass accumulation, P concentration and AMF symbiosis.

Table S1 Primer designed for gene silencing

Table S2 Genes and primers used in Real-time qPCR analysis

Fig. 1 Elevated CO_2 systemically induces strigolactone biosynthesis, AMF colonization and P uptake. (a) P accumulation per plant. (b) Root AMF colonization. (c) Transcript accumulation of strigolactone biosynthesis related genes in roots. Seedlings at 5-leaf stage grown in a sterilized soil/quartz sand/vermiculite mixture (1/1/1) were exposed to ambient atmospheric CO_2 (aCO_2, 380 ppmv) or elevated atmospheric CO_2 (eCO_2, 800 ppmv) for 28 d (a, b) or 10 d (c) in the presence of Rhizophagus irregularis AMF (+) or not (-) under P sufficient (+, 1 mM KH_2PO_4) or P deprivation (-, without KH_2PO_4 but with the addition of 1mM KCl) conditions. Data in (a) and (c) are mean±SD of three biological replicates. Different letters indicate significant difference at $P<0.05$.

Fig. 2 Shoot RBOH1 mediates CO_2-induced auxin signaling, AMF colonization and P uptake. (a-c) RBOH1 transcript (a), H_2O_2 accumulation in the apoplast (b), and IAA accumulation (c) in the leaves at the shoot apex. (d) DR5:GUS expression in the roots. (e, f) P accumulation in plants (e) and root AMF colonization (f) in grafted plants with RBOH1-RNAi (rboh) as scion (S) or rootstock (R). For (a-d), hydroponically-grown tomato plants at the 5-leaf stage were exposed to aCO_2 and eCO_2 with either P sufficient (1 mM KH_2PO_4) or P deficient (0.05mM KH_2PO_4 with the addition of 0.95 mM KCl) conditions for 1 d in controlled growth chambers. For (e and f), the grafted plants grown in a sterilized soil/quartz sand/vermiculite mixture (1/1/1) were exposed to aCO_2 or eCO_2 under P starvation (without KH_2PO_4 but with the addition of 1mM KCl) conditions in the presence of Rhizophagus irregularis for 28 d. FW, fresh weight. Arrows in (b) indicates H_2O_2-$CeCl_3$ precipitates. Data in (a), (c) and (e) are mean±SD of three biological replicates. AMF colonization in (f) was

scored from ca. 300 root/gridline intersects. Different letters indicate significant difference at $P<0.05$.

Fig. 3 Auxin signaling activates CO_2-induced biosynthesis of strigolactones, AMF colonization and P uptake. (a, b) P accumulation per plant (a) and root AMF colonization (b) in grafted plants grown in a sterilized soil/quartz sand/vermiculite mixture (1/1/1) with auxin-resistant diageotropica mutant (dgt) as scion (S) or rootstock (R) after exposure to ambient atmospheric CO_2 (aCO_2, 380 ppmv) or elevated atmospheric CO_2 (eCO_2, 800 ppmv) under P deprivation (without KH_2PO_4 but with the addition of 1mM KCl) conditions in the presence of Rhizophagus irregularis for 28 d. (c) Transcript accumulation of strigolactone biosynthesis and signaling related genes in roots of hydroponically-grown plants with dgt as scion (S) or rootstock (R) after exposure to aCO_2 or eCO_2 under P deficient (0.05 mM KH_2PO_4 with the addition of 0.95 mM KCl) conditions for 10 d. Data in (a) and (c) are mean±SD of three biological replicates. AMF colonization in (b) was scored from ca. 300 root/gridline intersects. Different letters indicate significant difference at $P<0.05$.

Fig. 4 Strigolactones are essential for CO_2-induced AMF colonization and P uptake. (a) P accumulation per plant. (b) Root AMF colonization. (c) Transcript of PT genes in roots. The CCD7, CCD8, MAX1 and MAX2-silencing plants grown in a sterilized soil/quartz sand/vermiculite mixture (1/1/1) were exposed to ambient atmospheric CO_2 (aCO_2, 380 ppmv) or elevated atmospheric CO_2 (eCO_2, 800 ppmv) in the presence of Rhizophagus irregularis under P deprivation (without KH_2PO_4 but with the addition of 1mM KCl) conditions for 28 d (a,b) or 10 d (c), respectively. Data in (a) and (c) are mean±SD of three replicates. AMF colonization in (b) was scored

from ca. 300 root/gridline intersects. Different letters indicate significant difference at $P<0.05$.

Fig. 5 A model for systemic eCO_2 signaling that promotes AMF symbiosis and associated P uptake. eCO_2 triggers an apoplastic H_2O_2 dependent production of auxin in the shoots followed by systemic induction of auxin signaling and resultant strigolactone biosynthesis in the roots of tomato plants. This signaling cascade enhances phosphate absorption by altering root system architecture (RSA) in the absence of AMF or facilitating mycorrhizal symbiosis in the presence of AMF.

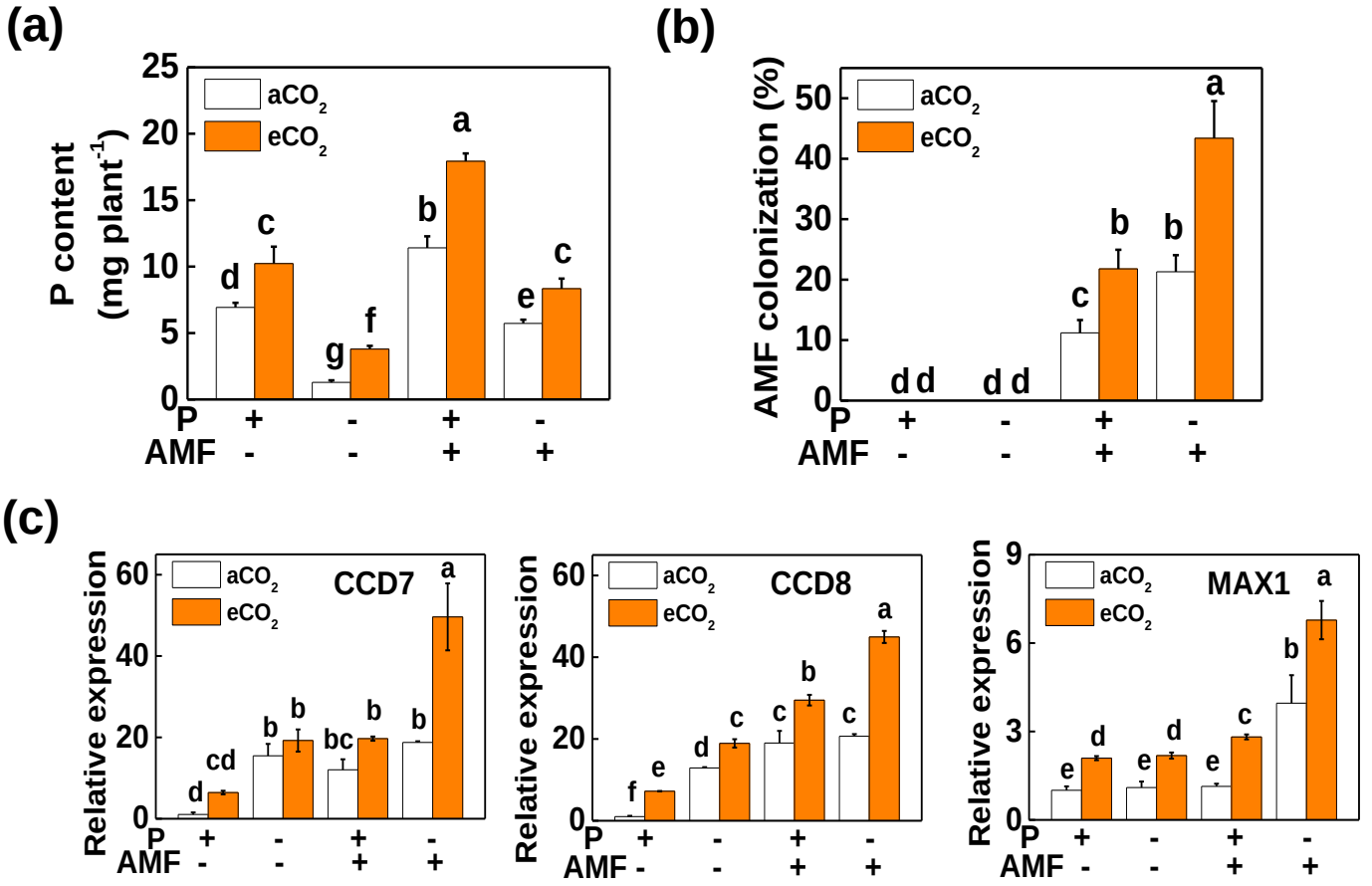
(a)
P content (mg plant-1)
aCO2
eCO2
P
AMF
(b)
AMF colonization (%)
(c)
Relative expression
CCD7
CCD8
MAX1

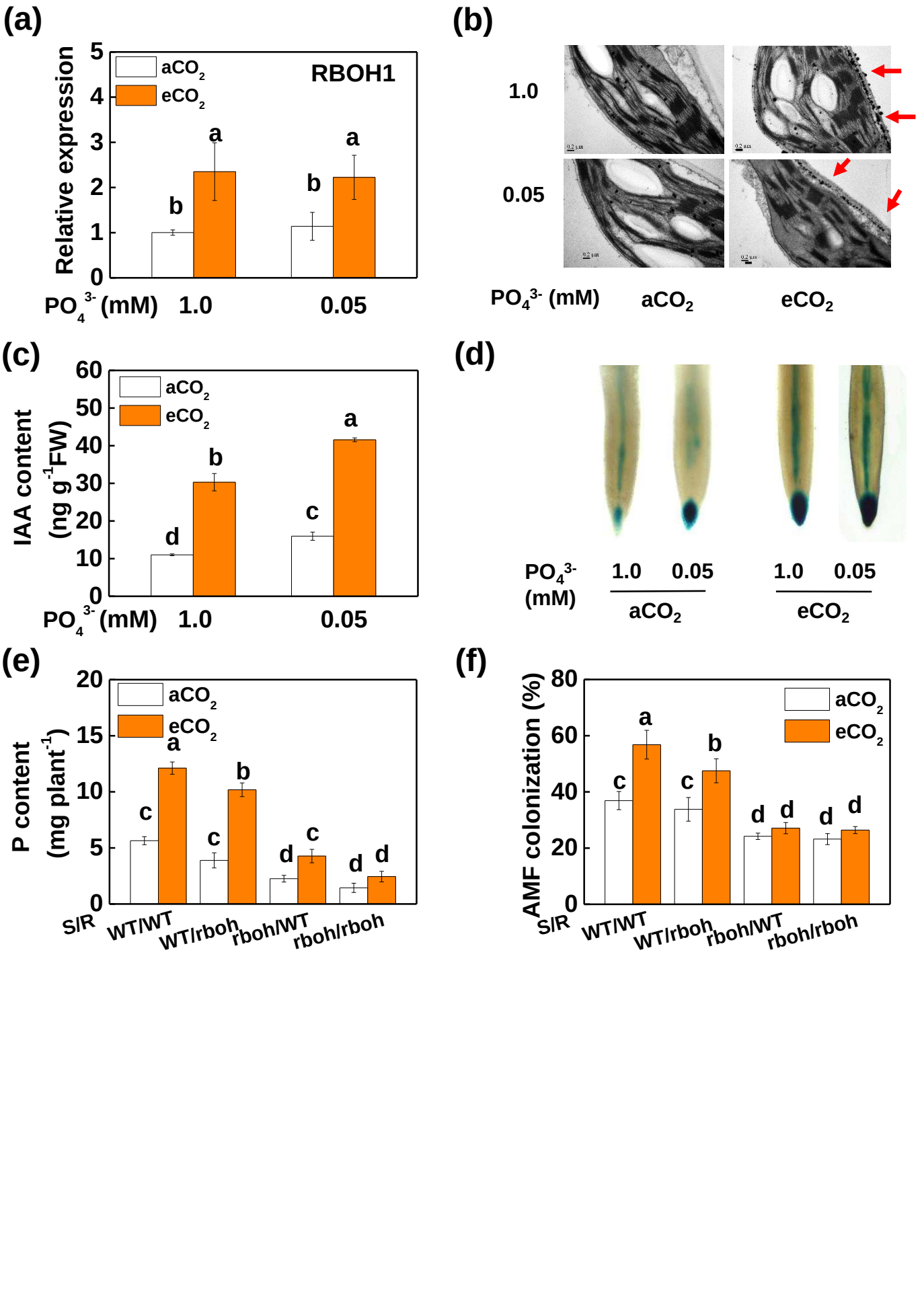
(a)
RBOH1
aCO2
eCO2
Relative expression
PO4 3- (mM) 1.0 0.05
(b)
1.0
0.05
PO4 3- (mM) aCO2 eCO2
(c)
IAA content (ng g-1FW)
PO4 3- (mM) 1.0 0.05
(d)
PO4 3- (mM) 1.0 0.05 1.0 0.05
aCO2 eCO2
(e)
P content (mg plant-1)
S/R WT/WT WT/rboh rboh/WT rboh/rboh
(f)
AMF colonization (%)
S/R WT/WT WT/rboh rboh/WT rboh/rboh

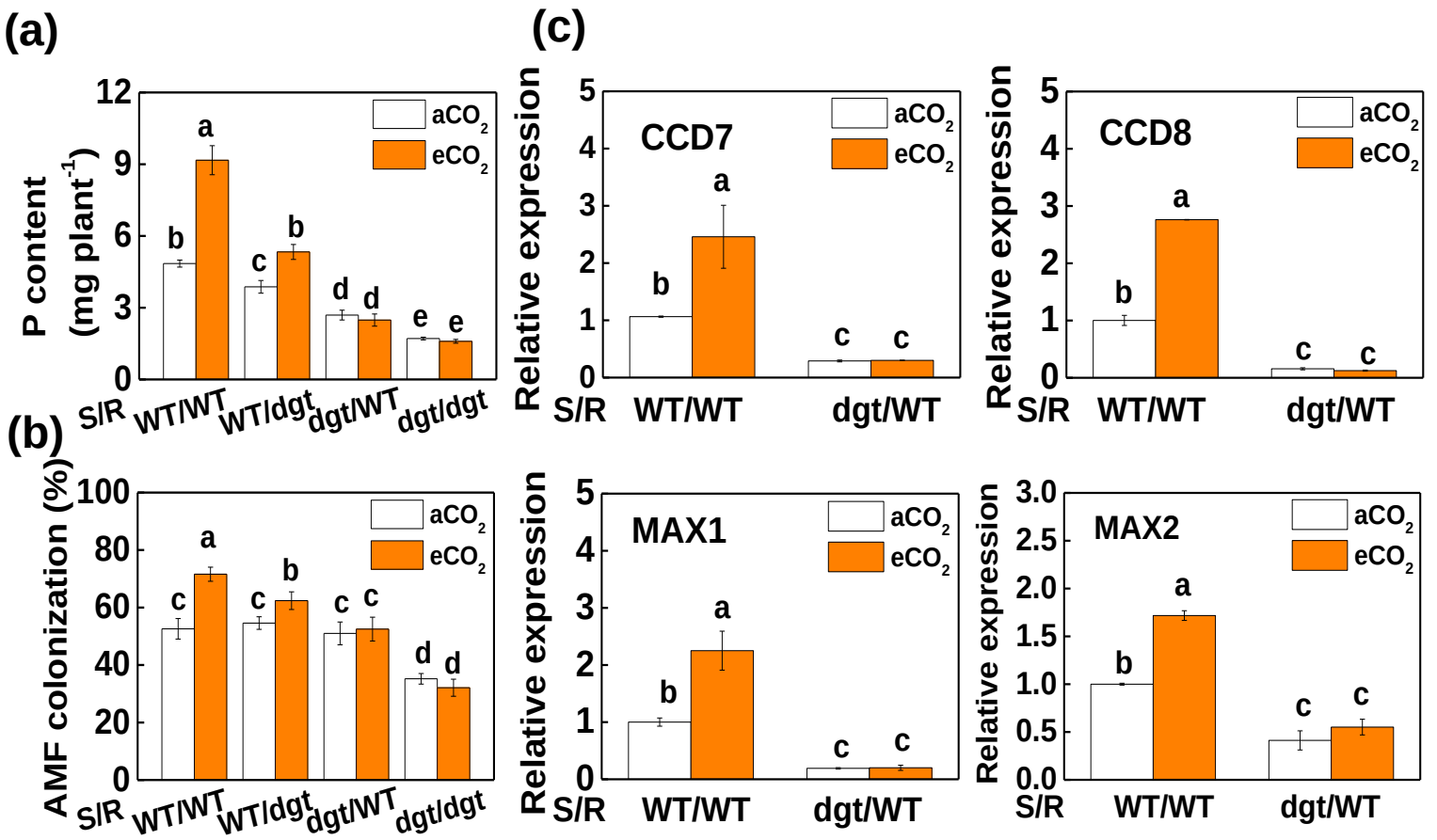
(a)
P content (mg plant-1)
aCO2
eCO2
S/R
WT/WT
WT/dgt
dgt/WT
dgt/dgt
(b)
AMF colonization (%)
(c)
CCD7
CCD8
MAX1
MAX2
Relative expression
dgt/WT

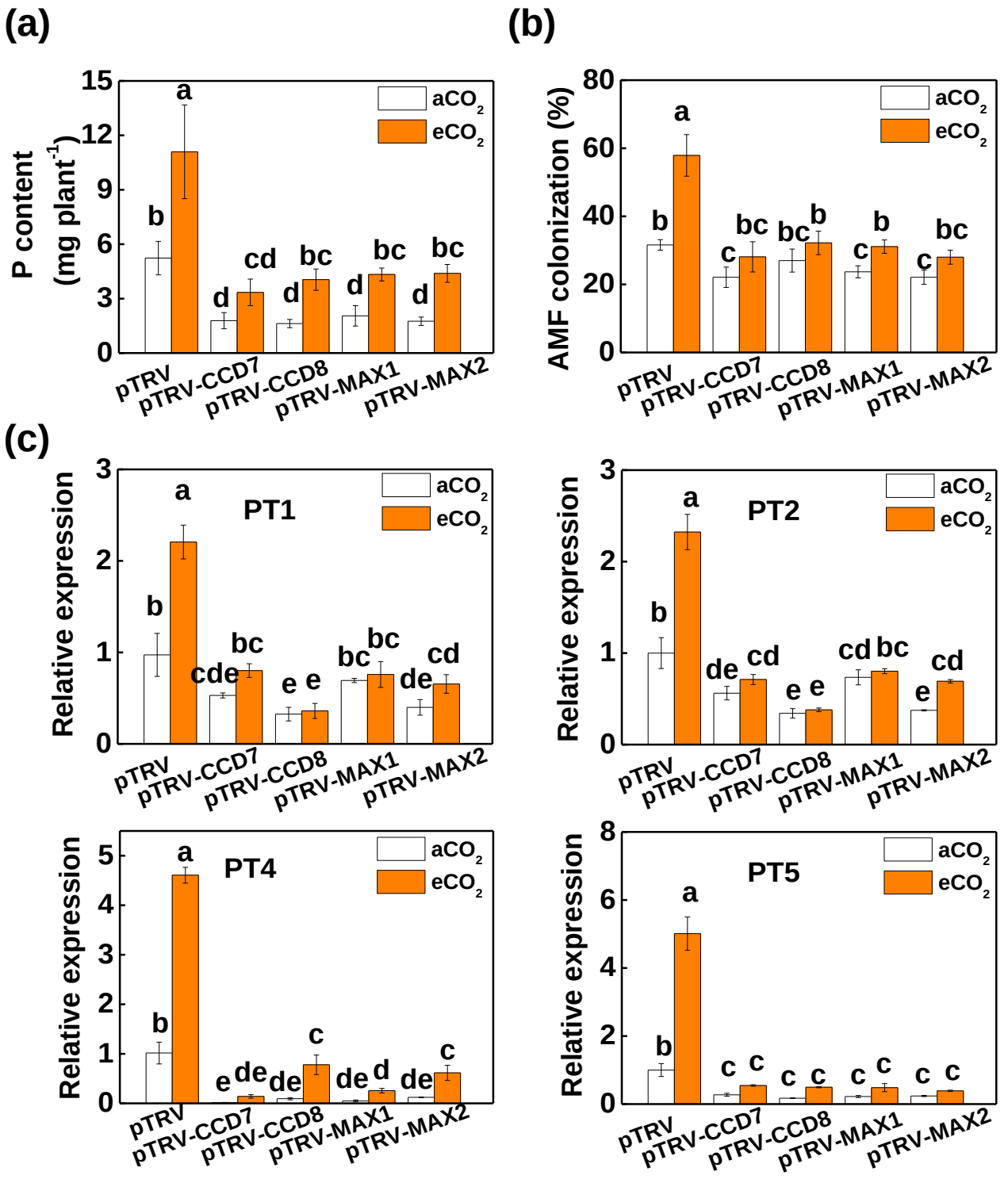
(a)
P content (mg plant-1)
aCO2
eCO2
pTRV
pTRV-CCD7
pTRV-CCD8
pTRV-MAX1
pTRV-MAX2
(b)
AMF colonization (%)
(c)
Relative expression
PT1
PT2
PT4
PT5

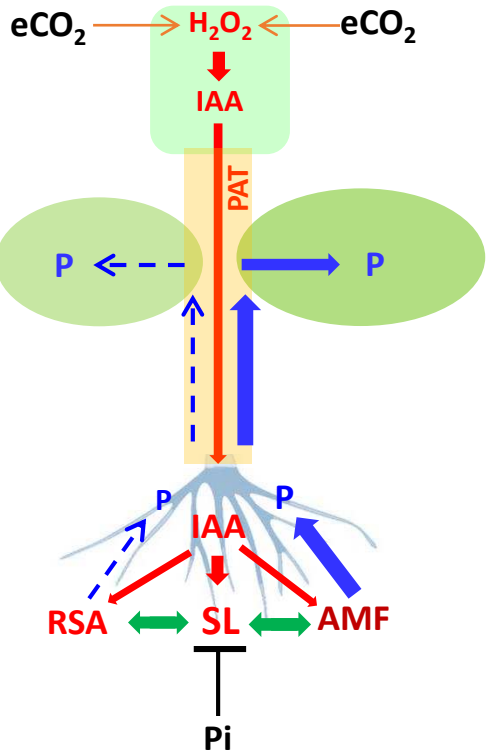
eCO2
H2O2
eCO2
IAA
PAT
P
P
P
P
IAA
RSA
SL
AMF
Pi

Fig. S1

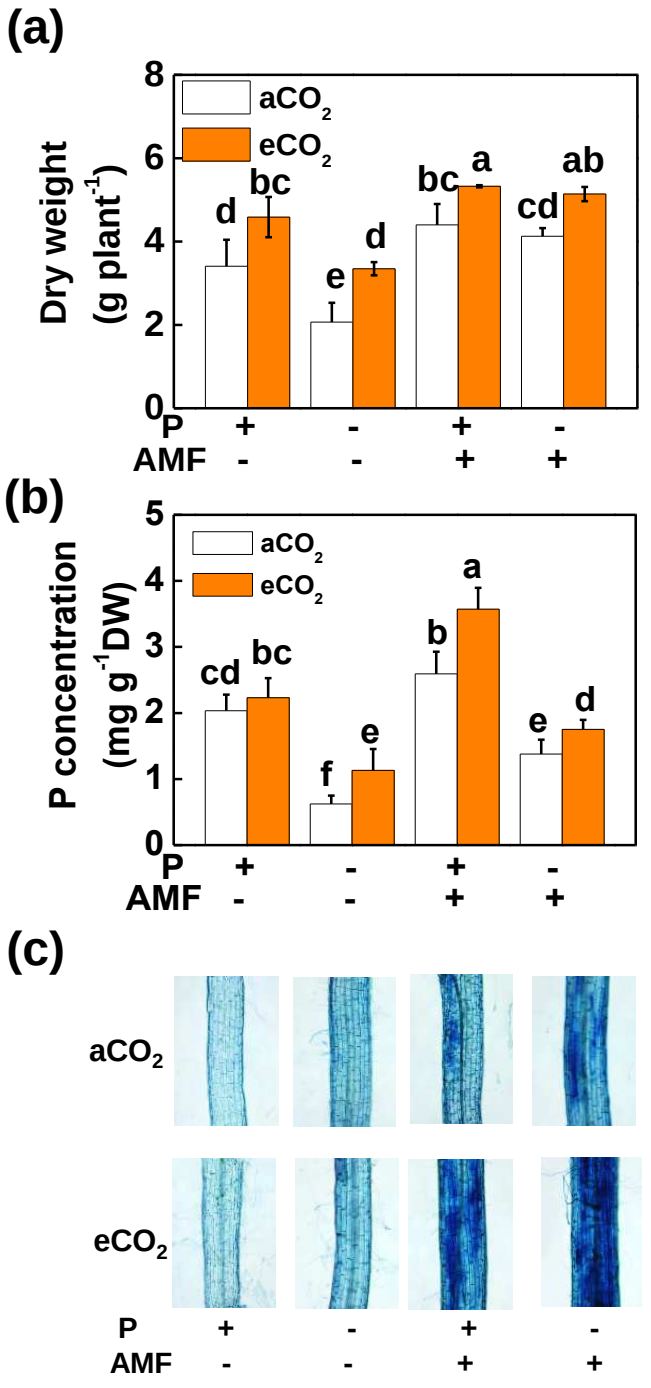
(a)
Dry weight (g plant-1)
aCO2
eCO2
d
bc
e
d
bc
a
cd
ab
P + - + -
AMF - - + +
(b)
P concentration (mg g-1DW)
aCO2
eCO2
cd
bc
f
e
b
a
e
d
P + - + -
AMF - - + +
(c)
aCO2
eCO2
P + - + -
AMF - - + +

Fig. S2

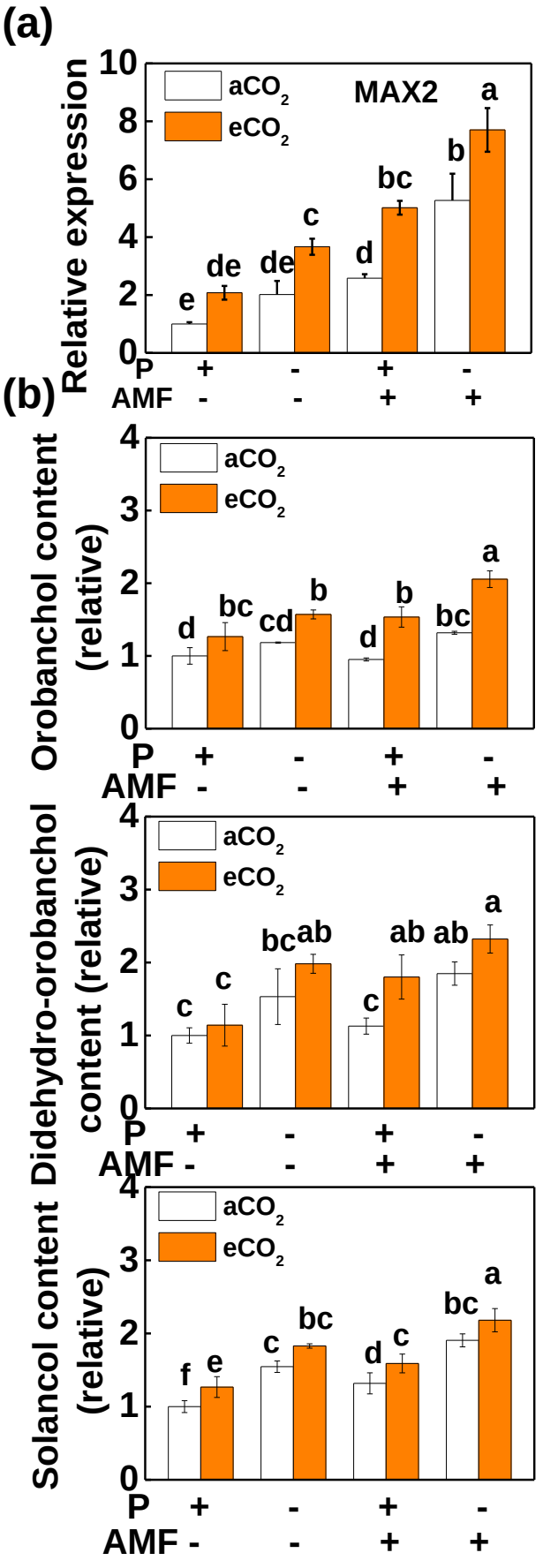
(a)
Relative expression
MAX2
aCO2
eCO2
e de de c d bc b a
P + - + -
AMF - - + +
(b)
Orobanchol content (relative)
d bc cd b d b bc a
Didehydro-orobanchol content (relative)
c c bc ab c ab ab a
Solancol content (relative)
f e c bc d c bc a

Fig. S3

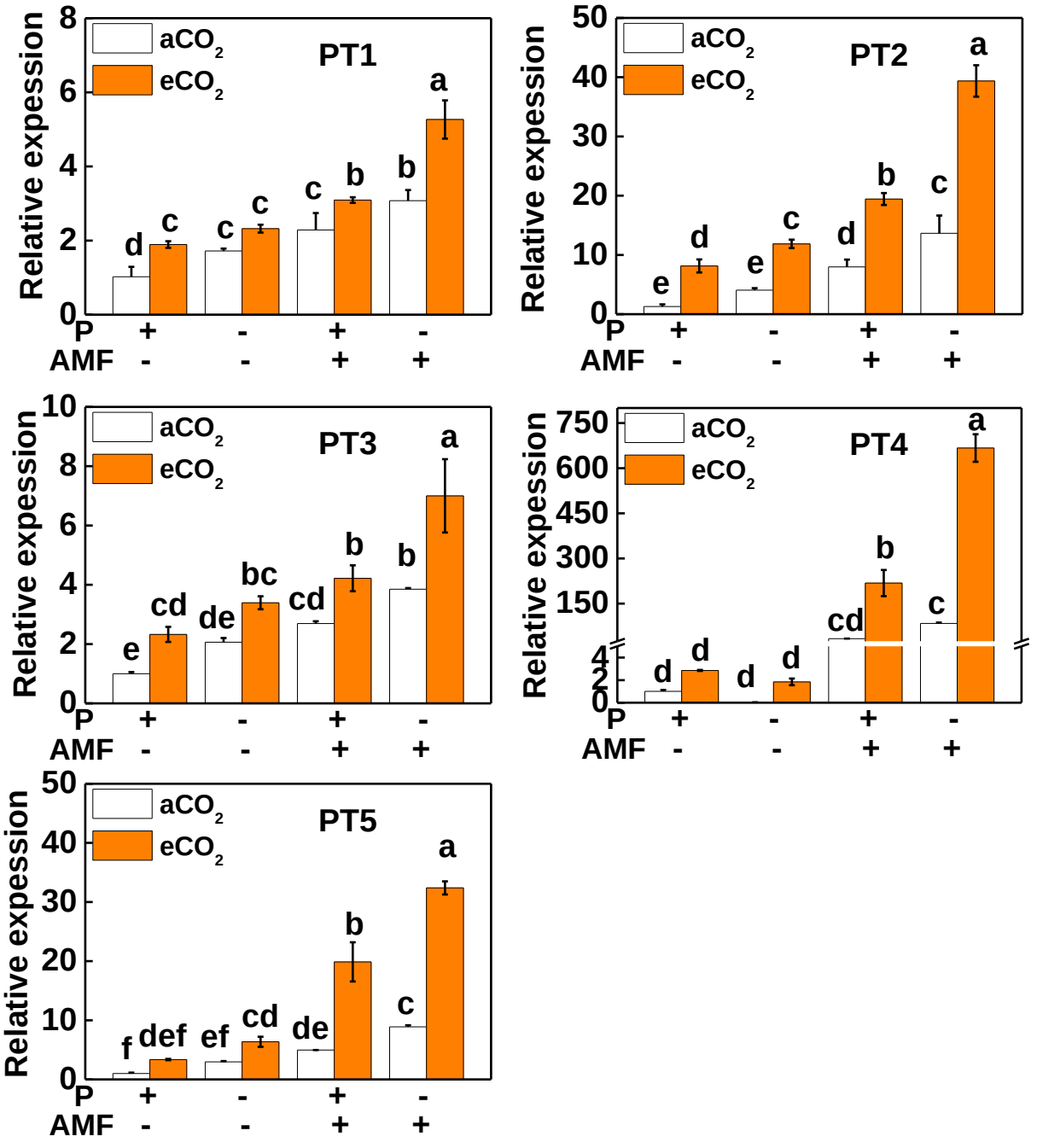

Fig. S4

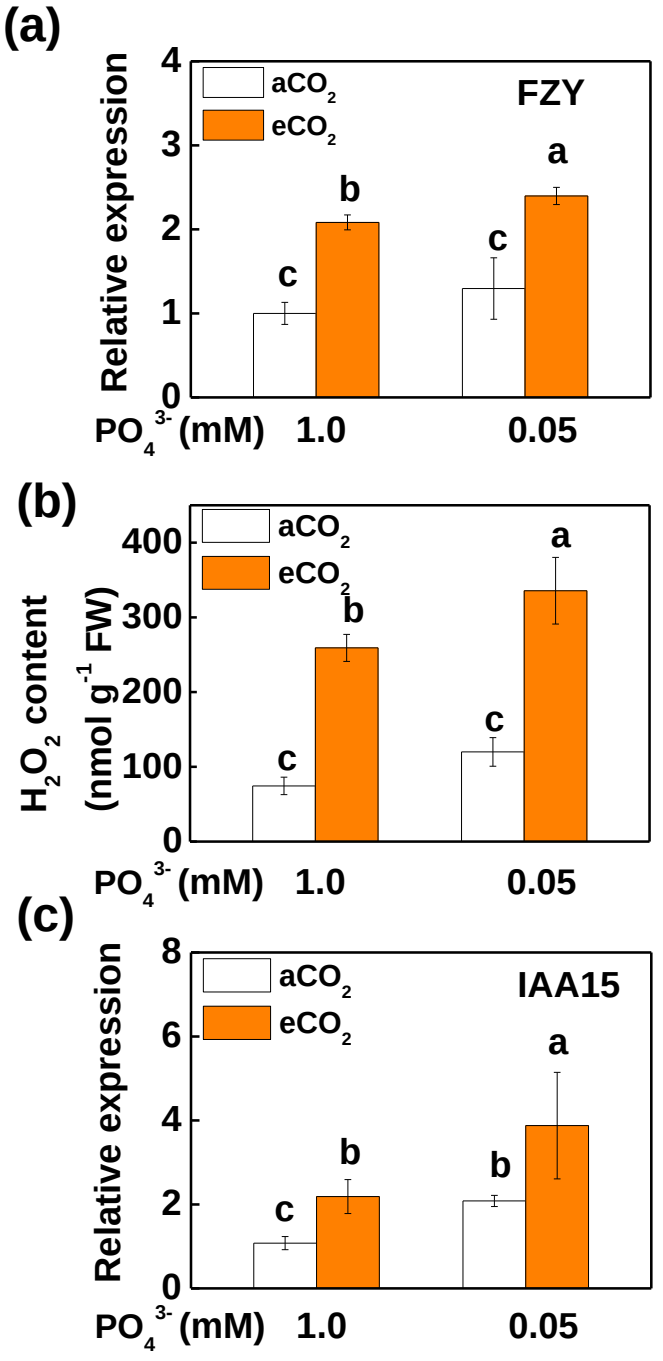
(a)
Relative expression
aCO2
eCO2
FZY
a
b
c
c
PO4 3- (mM) 1.0 0.05
(b)
H2O2 content (nmol g-1 FW)
aCO2
eCO2
a
b
c
c
PO4 3- (mM) 1.0 0.05
(c)
Relative expression
aCO2
eCO2
IAA15
a
b
b
c
PO4 3- (mM) 1.0 0.05

Fig. S5

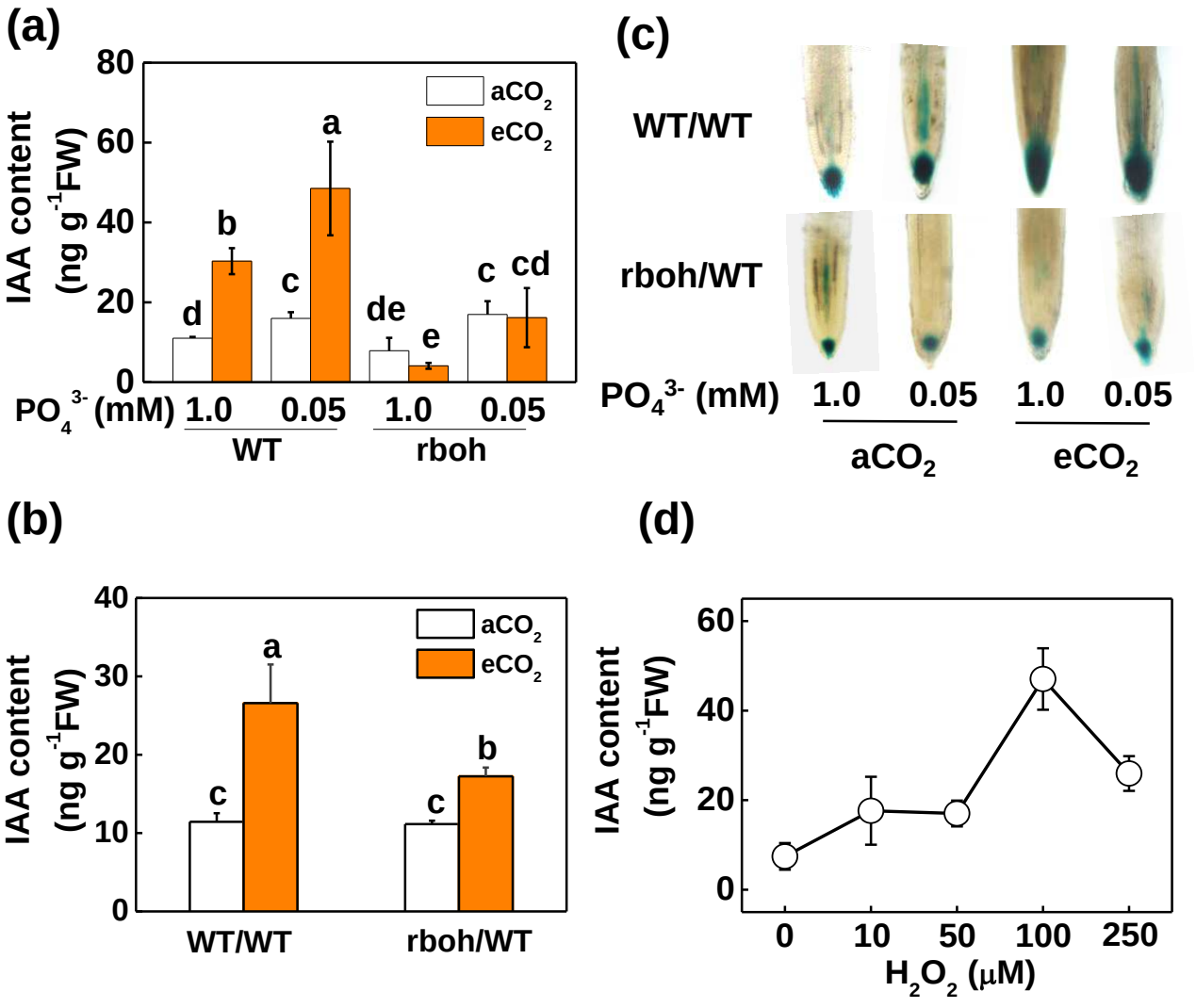
(a)
IAA content (ng g-1FW)
aCO2
eCO2
PO4 3- (mM) 1.0 0.05 1.0 0.05
WT
rboh
(c)
WT/WT
rboh/WT
PO4 3- (mM) 1.0 0.05 1.0 0.05
aCO2
eCO2
(b)
IAA content (ng g-1FW)
WT/WT
rboh/WT
(d)
IAA content (ng g-1FW)
H2O2 (μM)

Fig. S6

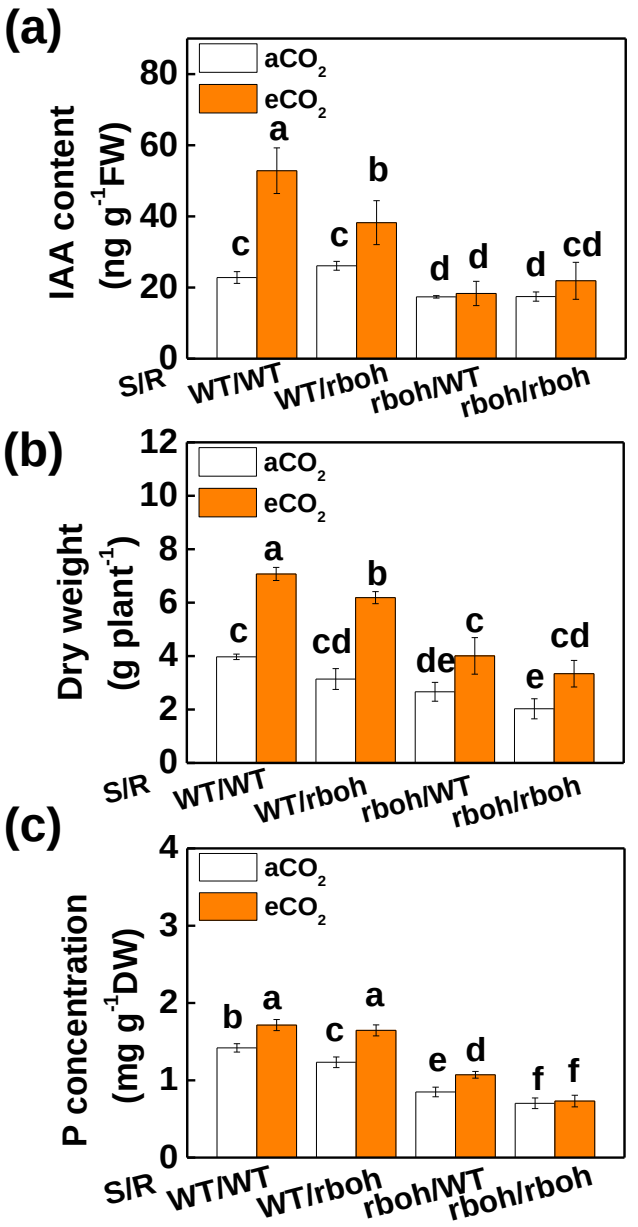
(a)
IAA content (ng g-1FW)
aCO2
eCO2
a
b
c
c
d
d
d
cd
S/R
WT/WT
WT/rboh
rboh/WT
rboh/rboh
(b)
Dry weight (g plant-1)
a
b
c
cd
de
c
e
cd
(c)
P concentration (mg g-1DW)
b
a
c
a
e
d
f
f

Fig. S7

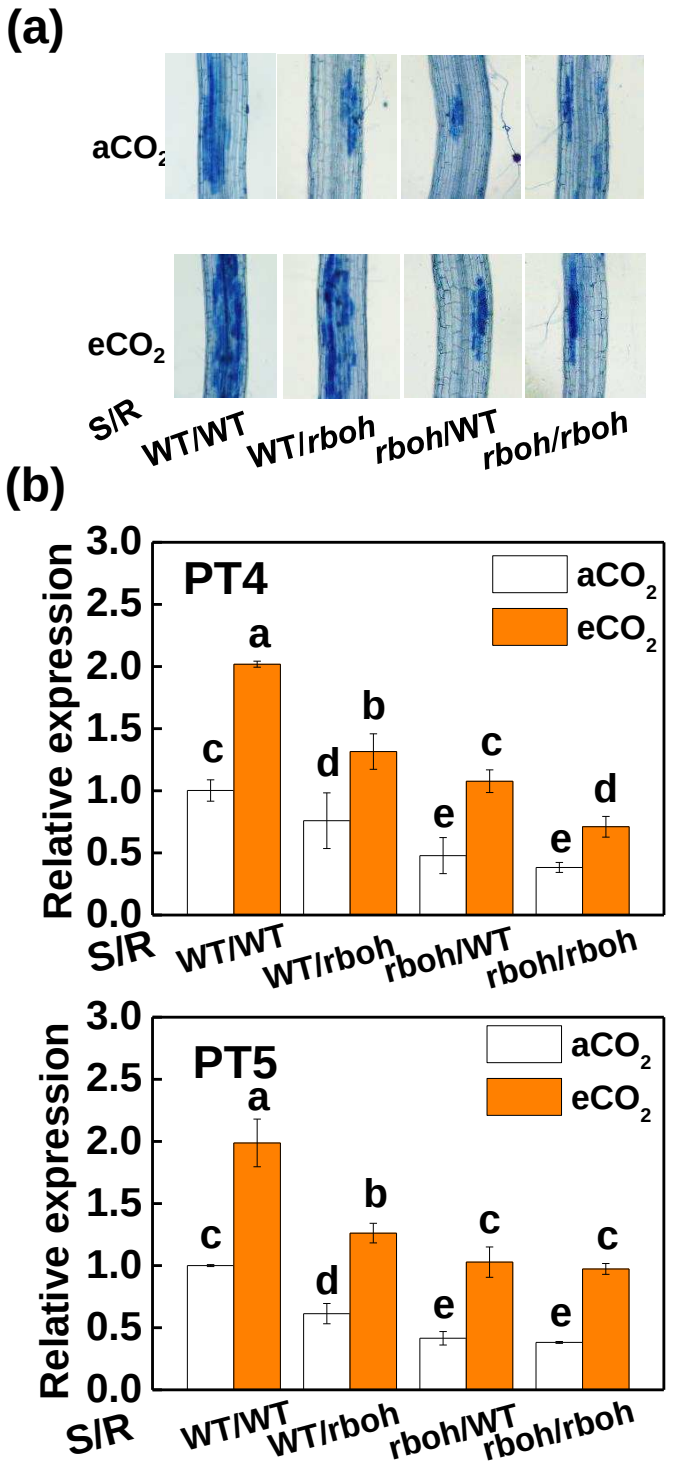
(a)
aCO2
eCO2
S/R
WT/WT
WT/rboh
rboh/WT
rboh/rboh
(b)
PT4
aCO2
eCO2
Relative expression
3.0
2.5
2.0
1.5
1.0
0.5
0.0
a
b
c
d
c
d
e
e
S/R
WT/WT
WT/rboh
rboh/WT
rboh/rboh
PT5
aCO2
eCO2
Relative expression
3.0
2.5
2.0
1.5
1.0
0.5
0.0
a
b
c
d
c
c
e
e
S/R
WT/WT
WT/rboh
rboh/WT
rboh/rboh

Fig. S8

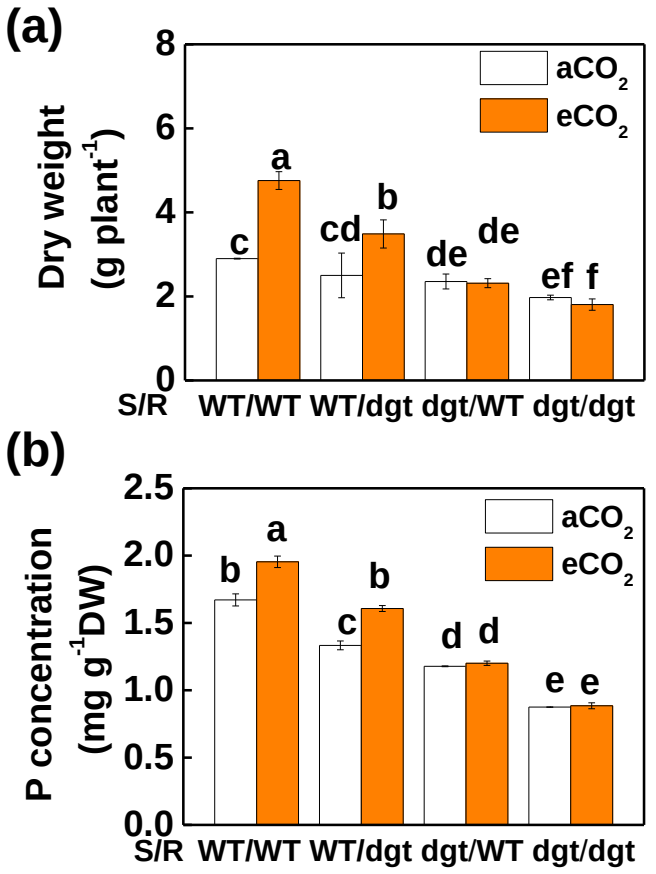
(a)
Dry weight (g plant-1)
8
6
4
2
0
aCO2
eCO2
a
b
c
cd
de
de
ef
f
S/R
WT/WT
WT/dgt
dgt/WT
dgt/dgt
(b)
P concentration (mg g-1DW)
2.5
2.0
1.5
1.0
0.5
0.0
aCO2
eCO2
b
a
c
b
d
d
e
e
S/R
WT/WT
WT/dgt
dgt/WT
dgt/dgt

Fig. S9

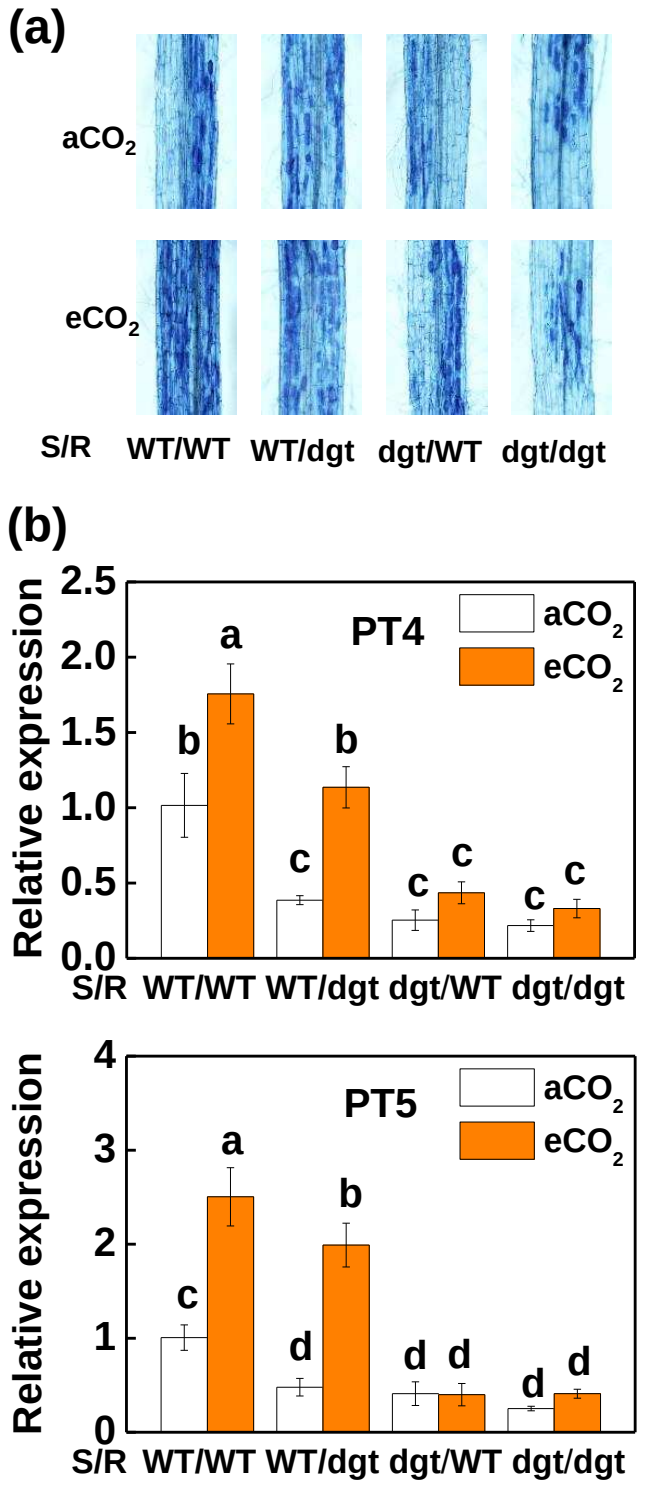
(a)
aCO2
eCO2
S/R WT/WT WT/dgt dgt/WT dgt/dgt
(b)
Relative expression
PT4
aCO2
eCO2
a
b
b
c
c
c
c
c
S/R WT/WT WT/dgt dgt/WT dgt/dgt
Relative expression
PT5
aCO2
eCO2
c
a
d
b
d
d
d
d
S/R WT/WT WT/dgt dgt/WT dgt/dgt

Fig. S10

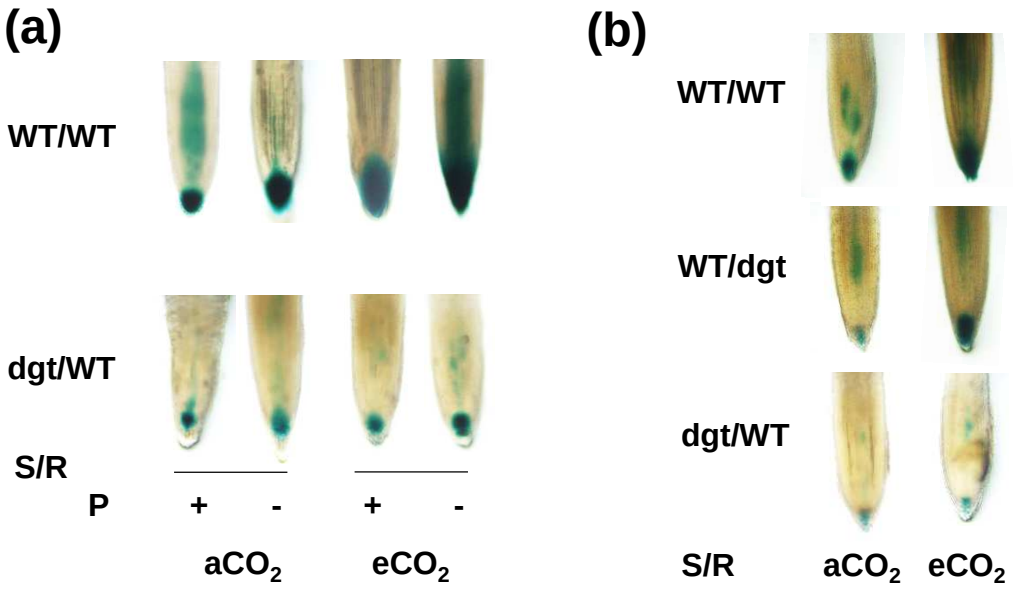

Fig. S10

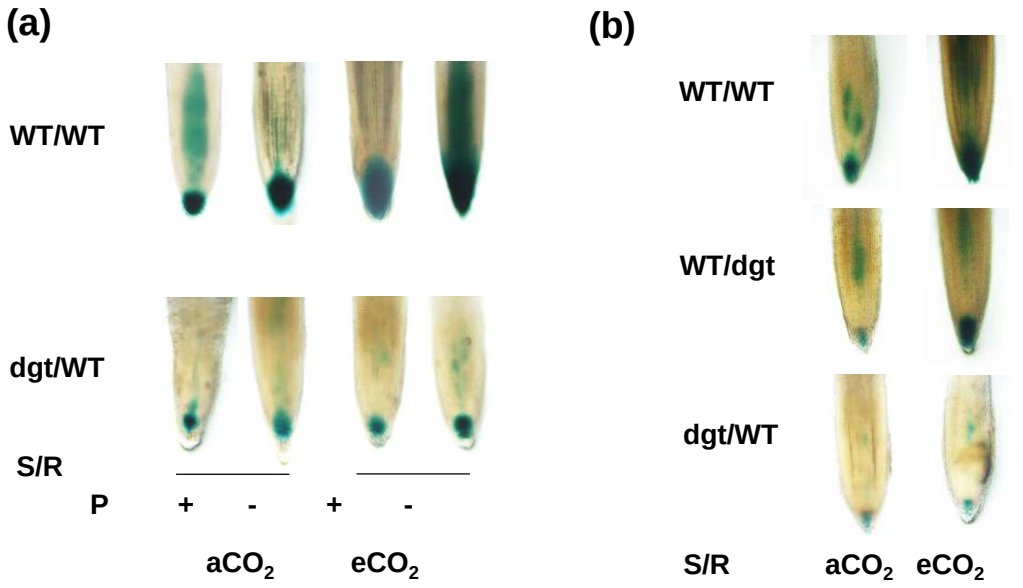

Fig. S11

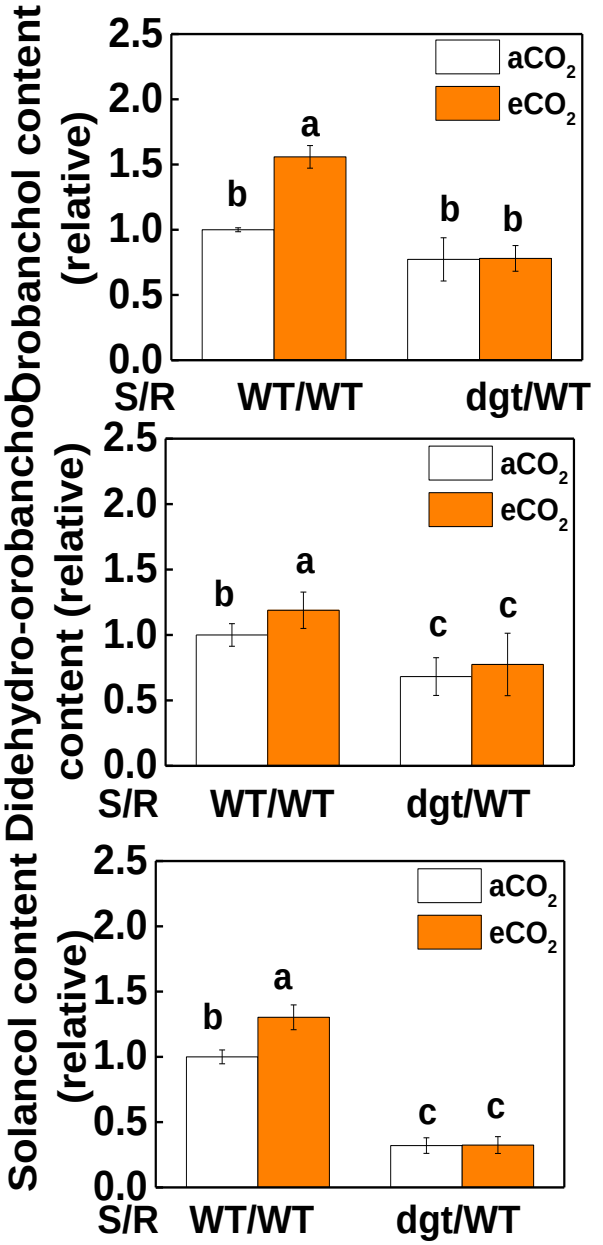
Solancol content Didehydro-orobanchol content Orobanchol content (relative)
2.5
2.0
1.5
1.0
0.5
0.0
aCO2
eCO2
a
b
b
b
S/R
WT/WT
dgt/WT
a
b
c
c
a
b
c
c

Fig. S12

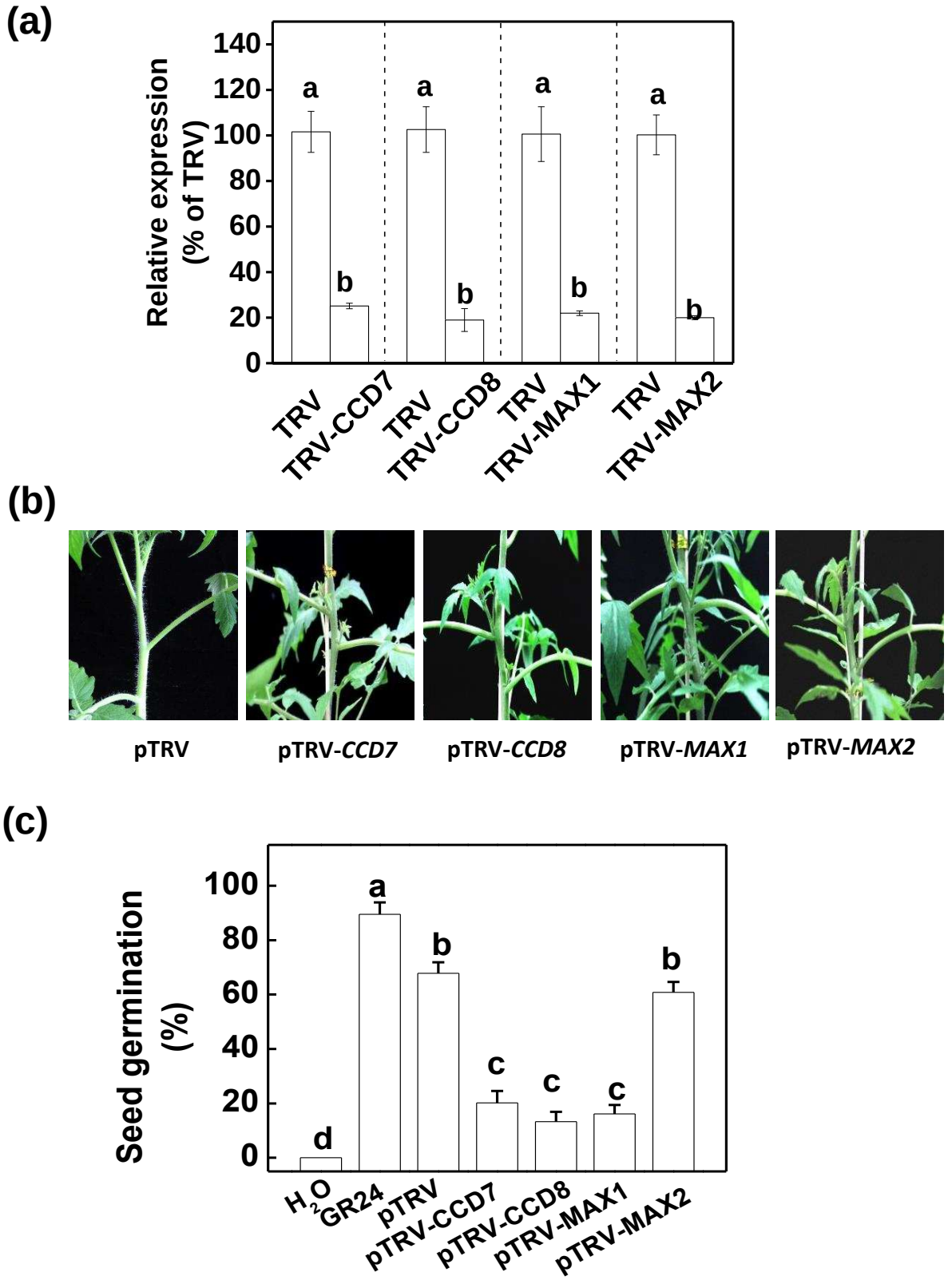
(a)
Relative expression (% of TRV)
140
120
100
80
60
40
20
0
a
b
a
b
a
b
a
b
TRV
TRV-CCD7
TRV
TRV-CCD8
TRV
TRV-MAX1
TRV
TRV-MAX2
(b)
pTRV
pTRV-CCD7
pTRV-CCD8
pTRV-MAX1
pTRV-MAX2
(c)
Seed germination (%)
100
80
60
40
20
0
d
a
b
c
c
c
b
H2O
GR24
pTRV
pTRV-CCD7
pTRV-CCD8
pTRV-MAX1
pTRV-MAX2

Fig. S13

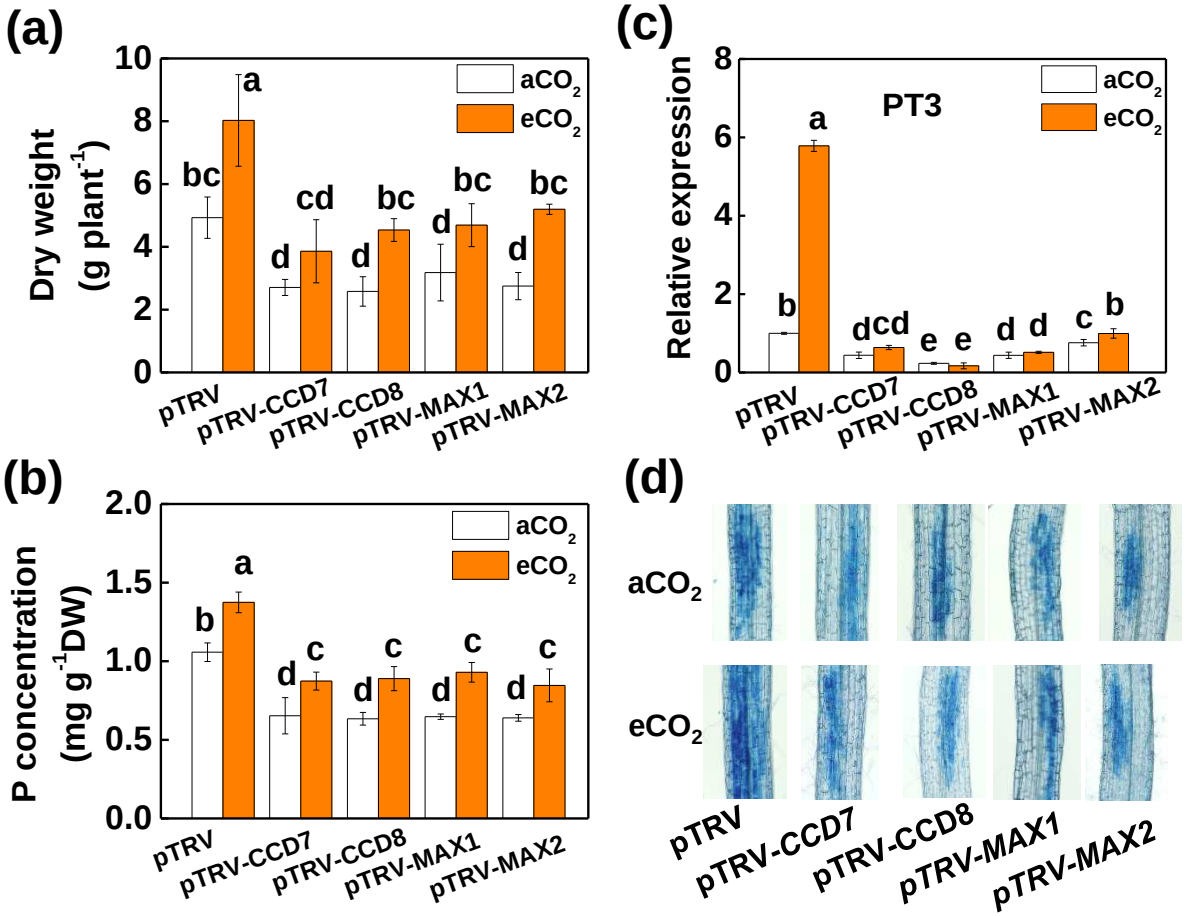
(a)
Dry weight (g plant-1)
aCO2
eCO2
pTRV
pTRV-CCD7
pTRV-CCD8
pTRV-MAX1
pTRV-MAX2
(b)
P concentration (mg g-1DW)
(c)
Relative expression
PT3
(d)
aCO2
eCO2